Photosynthetic Electron Transfer Controlled by Protein Relaxation: Analysis by Langevin Stochastic Approach

Dmitry A. Cherepanov,*† Lev I. Krishtalik,† and Armen Y. Mulkidjanian*‡

*Division of Biophysics, Faculty of Biology/Chemistry, University of Osnabrück, D-49069 Osnabrück, Germany, †A. N. Frumkin Institute of Electrochemistry, Russian Academy of Sciences, Leninskii prosp. 31, 117071 Moscow, Russia, and ‡A. N. Belozersky Institute of Physico-Chemical Biology, Moscow State University, 119899 Moscow, Russia

ABSTRACT Relaxation processes in proteins range in time from picoseconds to seconds. Correspondingly, biological electron transfer (ET) could be controlled by slow protein relaxation. We used the Langevin stochastic approach to describe this type of ET dynamics. Two different types of kinetic behavior were revealed, namely: oscillating ET (that could occur at picoseconds) and monotonically relaxing ET. On a longer time scale, the ET dynamics can include two different kinetic components. The faster one reflects the initial, nonadiabatic ET, whereas the slower one is governed by the medium relaxation. We derived a simple relation between the relative extents of these components, the change in the free energy (ΔG), and the energy of the slow reorganization Λ. The rate of ET was found to be determined by slow relaxation at $-\Delta G \leq \Lambda$. The application of the developed approach to experimental data on ET in the bacterial photosynthetic reaction centers allowed a quantitative description of the oscillating features in the primary charge separation and yielded values of Λ for the slower low-exothermic ET reactions. In all cases but one, the obtained estimates of Λ varied in the range of 70–100 meV. Because the vast majority of the biological ET reactions are only slightly exothermic ($\Delta G \geq -100$ meV), the relaxationally controlled ET is likely to prevail in proteins.

INTRODUCTION

Electron transfer (ET) reactions are abundant in chemistry and biology. According to contemporary views, thermal and quantum fluctuations of medium play a major role in ET (see Bixon and Jortner, 1999 for a recent review). By applying the Franck–Condon principle, Marcus has derived a relation between the activation energy of ET reaction, E_a, the reaction free energy, ΔG, and the energy of medium reorganization, λ (Marcus, 1956, 1964):

$$E_a = \tfrac{1}{4}\lambda(1 + \Delta G/\lambda)^2. \quad (1)$$

Using the close analogy between ET reactions and solid-state nonradiative processes, Levich and Dogonadze (1959) developed a quantum approach to ET reactions in polar medium and calculated the Franck–Condon factor for the electron exchange between two reactants. According to the perturbation theory, the electronic coupling of reactants is determined by square of the tunneling matrix element, $\mathbf{V}$, and the frequency $\omega_{el} = \mathbf{V}/\hbar$ is the intrinsic rate of the electron exchange due to the quantum tunneling. The electronic coupling decays, with the increasing distance between reactants, approximately as $\exp(-\beta R)$. The factor β varies in the range of 0.1–0.2 nm^{-1} in different chemical systems (Marcus and Sutin, 1985) and is close to 0.14 nm^{-1} in proteins (Moser et al., 1992). In the latter case, β can be modified by the protein secondary and tertiary structure (Gray and Winkler, 1996).

If the distance between reactants is small enough and ω_{el} is higher than the rate of medium relaxation, the ET is controlled by the solvent dynamics (the adiabatic regime). In this case, the rate constant of ET depends on the effective frequency of the solvent fluctuations, ω_{eff} (Dogonadze and Urushadze, 1971),

$$k_{ad} = (2\pi)^{-1}\omega_{eff}\exp(-E_a/k_BT). \quad (2)$$

In the alternative case, when the rate of solvent relaxation is faster than ω_{el} (the nonadiabatic limit), the rate constant of ET could be calculated by the first-order time-dependent perturbation theory (Marcus, 1964). In the high-temperature limit, this approach gives the equation (see, for example, Marcus and Sutin, 1985),

$$k_{na} = 2\pi\hbar^{-1}|\mathbf{V}|^2(4\pi\lambda kT)^{-1/2}\exp(-E_a/k_BT) = k_0 \cdot \exp(-E_a/k_BT). \quad (3)$$

In ordinary solvents, the medium relaxation is complete in several picoseconds. Correspondingly, all ET reactions that are slower than several picoseconds are usually treated as nonadiabatic ones. In highly viscous liquids, the relaxation modes could, however, determine the rate of fast ET reactions (see e.g., Barbara et al., 1992). The theoretical treatment of the ET dynamics affected by slow medium relaxation is based on the separation of fast (vibrational) and slow (reorientational) motions in the system. Thereby, the slow frictional motion in harmonic potentials can be described by a system of two coupled Smoluchowski equations with source interconversion terms (Zusman, 1980;

Received for publication 29 August 2000 and in final form 17 December 2000.

Address reprint requests to Armen Mulkidjanian, Abteilung Biophysik, Fachbereich Biologie/Chemie, Universitat Osnabrück, D-49069 Osnabruck, Germany. Tel.: 49-0541-9692871; Fax: 49-0541-9692870; E-mail: mulkidjanian@biologie.uni-osnabrueck.de.

0006-3495/01/03/1033/17 $2.00

Alexandrov, 1980; Yakobson and Burshtein, 1980; Ovchinnikova, 1981), an example of which is

$$\frac{\partial P_A}{\partial t} = \frac{\varepsilon_o \Delta^2}{\varepsilon_s \tau_D}\left[\frac{\partial^2 P_A}{\partial Q^2} + \frac{1}{k_B T}\frac{\partial}{\partial Q}\left(\frac{\partial U_A}{\partial Q}\cdot P_A\right)\right] - k_{AB}(Q)\cdot P_A + k_{BA}(Q)\cdot P_B, \quad (4)$$

$$\frac{\partial P_B}{\partial t} = \frac{\varepsilon_o \Delta^2}{\varepsilon_s \tau_D}\left[\frac{\partial^2 P_B}{\partial Q^2} + \frac{1}{k_B T}\frac{\partial}{\partial Q}\left(\frac{\partial U_B}{\partial Q}\cdot P_B\right)\right] - k_{BA}(Q)\cdot P_B + k_{AB}(Q)\cdot P_A. \quad (5)$$

Here, $P_A(Q, t)$ and $P_B(Q, t)$ are the densities of the probabilities to find the system in the initial and the final electron states, respectively, at a given value of the slow relaxation coordinate Q; k_{AB} and k_{BA} are the rate constants of the forward and backward nonadiabatic ET reactions at a given Q, ε_o and ε_s are the optical and static dielectric permittivities, respectively, τ_D is the Debye relaxation time, the parameter Δ is determined by the correlation function of the random process, $\langle Q(t)Q(0)\rangle = \Delta^2 \exp(-|t|/\tau)$, and U_A and U_B are the initial and final potential energies, respectively, as functions of the relaxation coordinate Q.

A more general diffusional Smoluchowski–Vlasov equation in the linear approximation has been derived by Calef and Wolynes (1983). The quantum mechanical treatment of the frictional ET in the one-mode approximation has been formulated by Garg et al. (1985). In this work, the Fokker–Plank extension of the Smoluchowski Eqs. 4 and 5 has been derived.

Significant efforts have been devoted to the solution of Eqs. 4 and 5. Using the Laplace transformation, Zusman (1980) has derived the expressions for the average rate constants of ET at an arbitrary value of the electron resonance integral **V**. In the subsequent work, the polar solvents with two Debye relaxation times have been considered (Zusman, 1988).

Marcus and coworkers have analyzed the particular case of strongly exothermic ET reactions, when the back reaction described by Eq. 5 can be neglected (Sumi and Marcus, 1986; Nadler and Marcus, 1987, 1988). They have found that the dynamical effects of solvent polarization lead generally to nonexponential kinetics of the ET. In a detailed study, Rips and Jortner (1987a, 1987b) have modeled the dynamical solvent effects on ET reactions by using the real-time path integral formalism and Liouville equation. These authors have derived the general expressions for the influence functionals of the medium in the Gaussian approximation and for the ET rate. The latter expression gives a general unified description of the high and low barrier reactions that covers both the nonadiabatic and the solvent-controlled adiabatic limits. Rips and Jortner (1988) have also obtained the numerical solution of Eqs. 4 and 5 for the low barrier reaction. An approximate solution of Eqs. 4 and 5 has been found by Zhu and Rasaiah (1991); it has been later generalized to include the non-Debye type of polarization and quantum effects (Zhu and Rasaiah, 1992, 1994). The approximate solution could be represented as a numerically solvable integral equation (Rasaiah and Zhu, 1993). A detailed solution of Eqs. 4 and 5 was obtained by Roy and Bagchi (1994) using the Green's function technique in the Laplace transformed space. The time-dependent probabilities $P_A(Q, t)$ and $P_B(Q, t)$ can be obtained in the framework of this approach by numerical integration. A comprehensive survey of the publications in this field may be found in several excellent reviews (Bagchi and Gayathri, 1999; Raineri and Friedman, 1999; Bixon and Jortner, 1999).

Contrary to polar liquids, the relaxation processes in proteins range from picoseconds to seconds (Frauenfelder et al., 1991; McMahon et al., 1998). Correspondingly, the relaxational control over ET might be even more widespread in biology than in chemistry. The possibility that a protein relaxation could determine the rate of biological ET reactions is well recognized (see e.g., the discussion in Takahashi et al., 1992; Peloquin et al., 1994; Krishtalik, 1995; Gray and Winkler, 1996; Holzwarth and Muller, 1996; Moser et al., 1997; Kotelnikov et al., 1998; Li et al., 2000). Still, to our best knowledge, no attempts to apply Eqs. 4 and 5 to experimental data on biological ET have been reported. A possible reason might be the mathematical complexity: even by using the almost analytical approaches offered in Rasaiah and Zhu (1993) and Roy and Bagchi (1994), one has to solve a system of two coupled partial differential equations to describe each kinetic trace. This task requires enormous numeric calculations. In addition, the application of Eqs. 4 and 5 to the ET in proteins is fundamentally constrained by the impossibility to treat proteins, because of their heterogeneity, as Debye dielectrics (Warshel and Russell, 1984). Proteins are rather characterized by a set of vibrational and relaxational modes ordered by the three-dimensional amino acid matrix. Particularly in the subpicosecond time scale, proteins reveal a complex coherent vibrational dynamics that can modulate the fast ET (Liebl et al., 1999; Vos and Martin, 1999). Such oscillatory dynamics cannot be described by the Smoluchowski Eqs. 4 and 5. Instead, it requires the application of more complex multidimensional Fokker–Plank equations. Their solution, however, seems to be beyond the capacity of the modern ET theory.

Thus, there is an obvious gap between the well-elaborated theory of ET in liquids and the practical studies of ET reactions in proteins. Here we tried to cover this gap by applying the alternative Langevin stochastic approach to the relaxationally controlled ET dynamics. Namely, we considered the same type of ET dynamics as in the pioneering works (Zusman, 1980; Alexandrov, 1980; Yakobson and Burshtein, 1980; Ovchinnikova, 1981), but, instead of using Smoluchowski equations, described it by the Langevin equations. The latter are complementary to the deterministic Fokker–Plank equations (see, e.g., Risken, 1996) and there-

fore allow straightforward description of the coherent vibrational effects in the ET dynamics. Although the general applicability of the Langevin approach to the description of ET reactions has been previously noted (Hynes, 1986), we failed to find any examples where this approach has been used to describe particular experimental data. The advantages of the Langevin approach are the usage of simple ordinary differential equations (instead of partial differential equations for the distribution functions of coordinates and velocities) and the absence of limitation on the number of relaxational modes. The disadvantage is the stochastic character of the dynamics, so that a large number of realizations should be performed in the case of numerical simulations. The modern PC, however, helps to cope with this difficulty.

We applied the developed approach to the experimental data on ET in the bacterial photosynthetic reaction centers. The Langevin approach allowed the quantitative description of the oscillating features in the primary charge separation and the estimation of the slow reorganization energy, Λ, of the low-exothermic ET reactions.

RESULTS AND DISCUSSION

Langevin formulation of ET dynamics in the effective potential

In the ET theory, the polar environment is usually either approximated by a thermal bath of harmonic oscillators (see, e.g., Levich and Dogonadze, 1959; Leggett et al., 1987) or is treated as a Debye-type dielectric (following the pioneering work of Zusman, 1980). It is noteworthy that the former approach neglects effects of solvent relaxation, whereas the latter one ignores solvent inertia. The Langevin equation approach allows a more general description of the solvent dynamics. This approach treats the effects of solvent inertia explicitly and therefore discriminates the processes of solvent reorganization and relaxation.

The simplest case of a single classical vibration mode (with effective mass m and frequency ω) being subjected to frictional and random (Langevin) forces can be written as

$$\ddot{q} + \gamma\dot{q} + \omega^2(q - q_0) = (2\gamma k_B T/m)^{1/2} F(t), \qquad (6)$$

where the shift of the equilibrium position, q_0, reflects the reorganization of the system due to the change in the charge state of the reactants. In the underdamped regime, the rate of mode reorganization is equal to the frequency ω, whereas the rate of relaxation is determined by the friction coefficient γ. According to the fluctuation–dissipation theorem, the amplitude of the random force $F(t)$ accounting for the Maxwellian velocity distribution is connected with the viscous friction coefficient γ so that $\langle F(t)\rangle = 0$ and $\langle F(t_1)F(t_2)\rangle = \delta(t_1 - t_2)$.

The nonadiabatic approach to ET implies a fast thermal equilibration of the oscillators both in the reactant and product states. In other words, the relaxation rate γ is assumed to be infinitely fast as compared to the intrinsic rate of electron transfer $\mathbf{V}/\hbar$ but much slower than the frequency of the oscillations ($\omega \gg \gamma \gg \mathbf{V}/\hbar$). The adiabatic approach to ET, that treats the solvent as a Debye-type dielectic, implies that the viscous friction γ is much faster than the self-frequency ω but slower than the rate of ET ($\omega \ll \gamma \ll \mathbf{V}/\hbar$). If the relation between ω, γ, and $\mathbf{V}/\hbar$ differs from these two extreme cases, neither of two these approaches could be applied to ET, whereas the Langevin approach remains valid.

In this work, we consider ET reactions that are partially or completely controlled by relaxation. Schematically, the mechanism of relaxational control over ET dynamics is depicted in Fig. 1, *A* (three-dimensional diagram) and *B* (two-dimensional cross-section). The fast motions in the system are visualized in this figure by the reaction coordinate q, whereas the slow motions proceed along the coordinate Q. The potential energy in the precursor electronic state A is shown by the left paraboloid in Fig. 1 *A* and by the left parabolic curves in Fig. 1 *B*. The product state B corresponds to the right paraboloid in Fig. 1 *A* and to the right parabolas in Fig. 1 *B*. The transition of the precursor state into the product one occurs at the intersection of two paraboloids. Due to the fast thermal motion along the coordinate q, the system reaches the transient configuration ($q_A^{\#}$, Q_A) at constant value of coordinate Q (*up arrow*). The following fast relaxation of the system along the coordinate q (*down arrow*) stabilizes the product state B only partially. The full stabilization requires also the rearrangement of the system along the slow coordinate Q (*white arrow*). It is noteworthy that, if the energy E_B^1 of the partially relaxed configuration (q_B, Q_A) is higher than the energy E_A^0 of the initial configuration (q_A, Q_A) (as it is shown in Fig. 1), the observable (measurable) ET kinetics are completely determined by the slow relaxation. Another remarkable feature of the system is that the forward and the back reactions go via different transition states, so that the back reaction does not represent an exact reversal of the forward one.

We approximated the vibrational characteristics of reactants and solvent by a large ensemble of linear oscillators with effective masses m_j and self-frequencies ω_j. The equilibrium position of an oscillator j was assumed to be zero in the precursor state A and to shift by δ_j in the product state B. Then the potential energy of the system in states A and B is

$$\begin{aligned} U_A &= \frac{1}{2}\sum_j m_j\omega_j^2 q_j^2, \\ U_B &= \frac{1}{2}\sum_j m_j\omega_j^2 (q_j - \delta_j)^2 + \Delta G^0, \end{aligned} \qquad (7)$$

where ΔG^0 is the free energy change of the reaction. It is impractical to define the microscopic parameters in detail. Instead we used a single "spectral function" $J(\omega)$ that can be expressed through the complex dielectric permittivity of the solvent (Garg et al., 1985; Leggett et al., 1987) or calculated

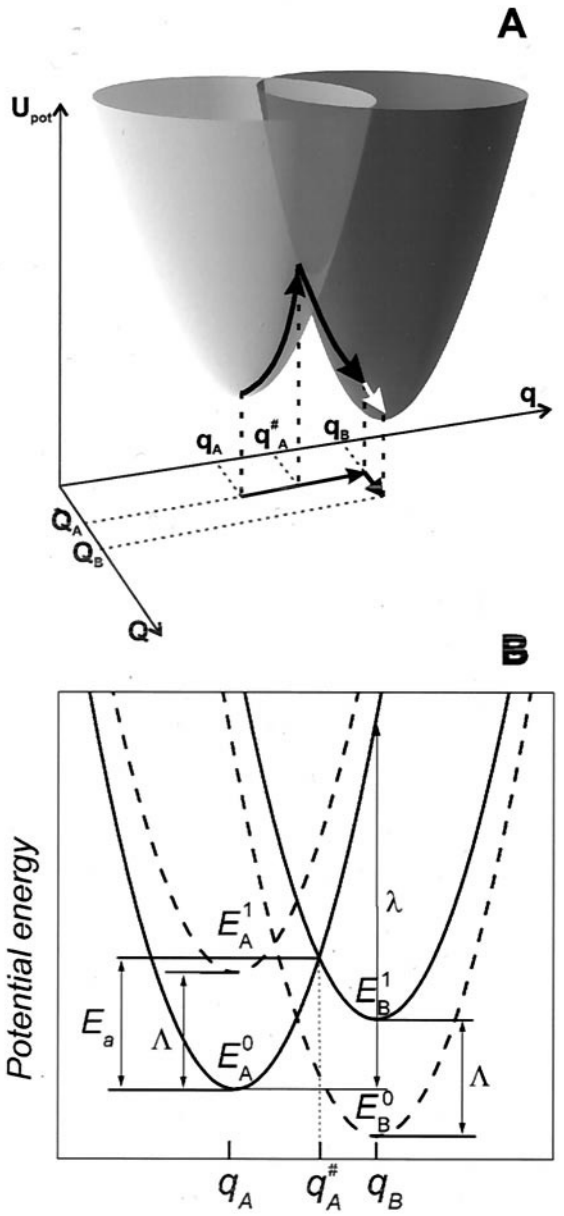

FIGURE 1 Scheme of a relaxationally controlled ET reaction. (*A*) Three-dimensional diagram. In the precursor state, the reactants are thermally equilibrated in the potential well A (*left surface*). The electron transition into the product state B (*right surface*) occurs at the intersection of two paraboloids during the thermal motion along the coordinate q at a constant value of the coordinate Q. (*B*) Two-dimensional cross-section of the energy diagram in (*A*). The parabolic potential energy profiles of the precursor (*left*) and product (*right*) electronic states are shown at two values of the relaxation coordinate Q: the solid curves are plotted at $Q = Q_A$, the dashed curves are plotted at $Q = Q_B$, respectively. See text for further details.

by methods of molecular dynamics (Warshel et al., 1989). We examined a special case of ET where $J(\omega)$ includes modes with frequencies Ω_j that are lower than the rate of electron exchange, $\Omega_j < k_{ET} = \min(k_{ad}, k_{na})$ (the rate constants of adiabatic, k_{ad}, and nonadiabatic, k_{na}, ET transitions are defined above by Eqs. 2 and 3, respectively).

The total reorganization energy could be separated thereby into the fast (λ) and slow (Λ) components (hereafter capital letters are used to discriminate the slower modes from the fast ones):

$$\lambda = \frac{1}{2}\sum_{\omega_j > k_{ET}} m_j\omega_j^2\delta_j^2, \quad \Lambda = \frac{1}{2}\sum_{\Omega_j < k_{ET}} M_j\Omega_j^2\Delta_j^2. \tag{8}$$

For convenience, we set $\Delta_j = 1$ in the product state. The slow modes were characterized then by the respective partial reorganization energies $\Lambda_j = \frac{1}{2}M_j\Omega_j^2$. At the long time scale, the energy gap between precursor and product states is a function of the coordinates Q_j and could be found by averaging the potential energy over the fast coordinates q_j,

$$\Delta G\{Q\} = \bar{U}_B\{Q\} - \bar{U}_A\{Q\} = \Delta G^0 + \sum_j \Lambda_j(1 - 2Q_j), \tag{9}$$

where the symbol $\{Q\}$ represents a parametric dependence on the whole multitude of slow coordinates Q_j. By using the theory of spin-boson Hamiltonian (Leggett et al., 1987), the general expressions for the transition rate constants k_{AB} and k_{BA} of the forward and reverse nonadiabatic ET, respectively, could be found (see Appendix A for a detailed consideration). In the high-temperature limit, the rate constants could be written in the simple form,

$$\begin{aligned} k_{AB}\{Q\} &= k_0\exp(-E_a\{Q\}/k_BT), \\ k_{BA}\{Q\} &= k_0\exp((\Delta G\{Q\} - E_a\{Q\})/k_BT), \end{aligned} \tag{10}$$

where the activation energy $E_a\{Q\}$ is defined by Eq. 1. The rate of adiabatic ET is defined by Eq. 2, where ω_{eff} could be found by integration of the spectral function (see, e.g., Kuznetsov, 1989). We denoted the probabilities to find the system at time t in states A or B as functions $P_A(t)$ and $P_B(t)$, respectively. At the short time scale, the time evolution of $P_A(t)$ and $P_B(t)$ was then governed by the kinetic equations,

$$\begin{aligned} \dot{P}_A(t) &= -k_{AB}\{Q\}\cdot P_A + k_{BA}\{Q\}\cdot P_B, \\ \dot{P}_B(t) &= k_{AB}\{Q\}\cdot P_A - k_{BA}\{Q\}\cdot P_B, \end{aligned} \tag{11}$$

that describe the initial exponential evolution to the steady-state Boltzmann probabilities $\bar{P}_A$ and $\bar{P}_B$:

$$\begin{aligned} \bar{P}_A &= (1 + \exp(-\Delta G\{Q\}/k_BT))^{-1}, \\ \bar{P}_B &= (1 + \exp(\Delta G\{Q\}/k_BT))^{-1}. \end{aligned} \tag{12}$$

The dynamics of slow reaction coordinates $\{Q\}$ was formulated in terms of Langevin stochastic differential equations. Here, the microscopic state of the system was represented by a point moving along a stochastic trajectory $\{Q(t)\}$ on the multidimensional surface of the effective potential $U\{Q\}$ that can be found by averaging the total energy of the system in the configuration space of fast coordinates (see

Appendix B for details):

$$U\{Q\} = -kT \ln\left[\exp\left(-\sum_j \frac{2\Lambda_j Q_j^2}{2k_B T}\right) + \exp\left(-\sum_j \frac{2\Lambda_j (Q_j - 1)^2 + \Delta G^0}{2k_B T}\right)\right]. \quad (13)$$

Substituting the first derivatives of $U\{Q\}$ into the Langevin equations, we come to the system of stochastic differential equations for the multitude of variables Q_j,

$$\ddot{Q}_j + \Gamma_j \dot{Q}_j + \Omega_j^2 [Q_j \cdot \bar{P}_A + (Q_j - 1) \cdot \bar{P}_B] = \sqrt{\Gamma_j k_B T \Omega_j^2 / \Lambda_j} F_j(t). \quad (14)$$

Here, three terms in the left part describe the inertial, viscous, and effective potential forces, respectively, the Langevin random forces $F_j(t)$ are defined similarly as in Eq. 6. The usage of the effective potential $U\{Q\}$ implies that the kinetics determined by Eq. 11 are much faster than those described by Eq. 14, so that the probabilities of the precursor and the final states $\bar{P}_A$ and $\bar{P}_B$ obey the Boltzmann distribution, Eq. 12. This restriction, however, could be weakened by using functions $P_A(t)$ and $P_B(t)$ instead of $\bar{P}_A$ and $\bar{P}_B$ and by solving Eqs. 11 and 14 together. Thereby the unified description of the relaxationally controlled ET was achieved.

Similar to the behavior of a harmonic oscillator, the solution of Eq. 14 reveals underdamped (oscillatory) and overdamped (monotonically relaxing) regimes of ET dynamics. Which of them is realized depends on the ratio between the damping factor, Γ_j (the rate of microscopic viscous relaxation) and the self-frequency Ω_j (the reorganization velocity).

At $\Gamma_j < \Omega_j$, oscillatory features could appear in the kinetics of ET. How wide is the time window where oscillations in ET could be expected? The frequency of the fastest collective vibrations (librations) in proteins is the same as in polar solvents and falls in the range of 300–3000 cm^{-1} (τ of 10–100 fs). For example, the OH-stretch vibration in water has the frequency of 3300 cm^{-1} (10 fs). The relaxation of this mode, as determined by polarization-resolved vibrational pump-probe spectroscopy (Woutersen and Bakker, 1999), proceeds, however, much slower, at 40 cm^{-1} (740 fs). In proteins, the difference between the relaxation and reorganization rates is even more pronounced. For instance, the stretch vibration of carbon monoxide bound to different forms of myoglobin has the frequency of 2100 cm^{-1} ($\tau \sim 16$ fs), whereas the relaxation of this mode, as measured by ultrafast time-resolved IR spectroscopy (Sagnella et al., 1999) and also calculated by molecular dynamics simulations (Sagnella and Straub, 1999), proceeds at 0.06–1.5 cm^{-1} (20–500 ps). It is noteworthy that librations proper give only a small contribution (~10%) to the total reorganization as judged from the dielectric response function (Hasted, 1973) and from the long-track molecular dynamics calculations (Gonzalez et al., 2000). The main contribution originates from the reorientational dynamics of dipoles (Debye-type polarization). In polar solvents the latter has a broad peak at 0.2–3 cm^{-1} (10–150 ps) (Hasted, 1973). Molecular dynamics simulations show that, in proteins, the reorientational dynamics is essentially slower, falling in the frequency range of 0.005–0.02 cm^{-1} (150–5000 ps) (Loffler et al., 1997). Because this type of polarization is purely relaxational and damps any types of oscillations, coherent effects with $\tau \geq 100$ ps are unlikely in proteins.

For further understanding, it is important to note that the same stochastic thermal collisions that are responsible for energy dissipation provide the energy input that is required to overcome the activation barrier of a ET reaction. If the dissipative processes are slower than the rate of electron exchange, $\mathbf{V}/\hbar$, the total energy of the system would not change, although the potential energy would vary with a frequency of some tens of femtoseconds. Then a minor fraction of reactants, with energy sufficient for ET, would randomly oscillate between precursor and product states, whereas in the rest of the ensemble ET would not proceed. Thus, ET cannot be faster than the fastest relaxation modes in the system. As a consequence: 1) ET in proteins can hardly proceed in the subpicosecond time scale; and 2) the nonadiabatic approximation that implies infinitely fast equilibration in the system can hardly be applied to biological ET reactions that are faster than 10 ps.

In the case of high friction, $\Gamma_j > \Omega_j$, Eq. 14 predict a monotonic behavior. For picosecond ET reactions, a number of kinetic components corresponding to different relaxation modes is expected (adiabatic regime). On a longer time scale, where the nonadiabatic approximation makes sense, the ET dynamics include two types of kinetic components. The faster, initial component is caused by the nonadiabatic ET at fixed coordinates $\{Q\}$, whereas the slower ones are connected with the further relaxation in the effective potential $U\{Q\}$. The rate constant of the fast ET component is just the sum of the forward and the backward rate constants in Eq. 10, whereas the kinetics of the slow component(s) are determined by the diffusion over an activation barrier that separates the precursor and the product potential wells (see Appendix B). If $\Lambda \geq k_B T$ and $\Lambda \geq -\Delta G$, the height of the barrier, U_{max}, can be approximated as $U_{max} = \frac{1}{4}\Lambda + \frac{1}{2}\Delta G$. Generally the diffusion over a potential barrier is nonexponential. However, in the limiting cases of the high and the low barriers, respectively, the kinetics of relaxation are monoexponential:

1. if $U_{max} \gg k_B T$, the rate constant of relaxation could be derived by the Kramer's escape rate theory (Hänggi et al., 1990), so that $k_{slow} = (2\pi\Gamma)^{-1} \Omega_{eff} \Omega_b \cdot \exp(-U_{max}/k_B T)$, where Ω_{eff} is the effective frequency of slow

modes, and Ω_b is the oscillator frequency at the top of the potential barrier;

2. if $U_{max} \leq k_B T$, the system can move almost freely in the effective potential and $k_{slow} = \Omega_{eff}^2 \Gamma^{-1}$. In the latter case, the rate of ET should be independent of ΔG and of the reorganization energy.

The relative amplitudes of the initial nonadiabatic and the subsequent relaxational components of ET kinetics could be calculated, in accordance with the Boltzmann statistical distribution, by using the value of the nonequilibrium energy gap, as given by Eq. 9:

$$\begin{aligned} A_{fast} &= (1 + \exp((\Delta G^0 + \Lambda)/k_B T))^{-1}, \\ A_{slow} &= (1 + \exp(-(\Delta G^0 + \Lambda)/k_B T))^{-1} \\ &\quad - (1 + \exp(-\Delta G^0/k_B T))^{-1}. \end{aligned} \tag{15}$$

It follows from Eqs. 15, that the contribution of the relaxational component becomes remarkable at $-\Delta G^0 \leq \Lambda$, and that the ratio between A_{fast} and A_{slow} depends on ΔG^0. Provided that ΔG^0 of biological ET reactions could be experimentally varied (see the following sections), the latter dependence could help to find out whether experimentally measured nonexponential ET kinetics are due to a relaxationally controlled ET. Alternatively, nonexponential kinetics could be attributed either to the structural heterogeneity of the protein (see e.g., Kleinfeld et al., 1984; McMahon et al., 1998) or to some "gating" mechanisms (see e.g., Graige et al., 1998; Sharp and Chapman, 1999). In the former case, an ensemble of more or less "frozen" conformational substates with differing intrinsic ET rates is invoked to explain the kinetic heterogeneity. In such a case, the relative extents of kinetic components are not expected to depend on ΔG^0. The gating concept implies that some slower reaction can hamper ET completely or partly. In a trivial case, the ET rate could be controlled by a genuine diffusion of a redox protein or by a conformational change (domain movement) that brings the redox centers together (the iron-sulfur Rieske protein in the cytochrome-bc_1 complex can serve as an illustrative example [Crofts et al., 1999]). In such a case, no dependence on ΔG^0 could be expected for the relative extents of kinetic components. Otherwise, an ET reaction could be gated (e.g., by a proton or substrate binding or by some conformational transition), although the distance between reactants stays invariably short (see Sharp and Chapman [1999] for a survey of representative examples). In such a case, it is possible to speak about thermodynamic coupling. Not surprisingly, many gated reactions of this type are involved in energy transduction. This kind of gating is physically equivalent to a relaxational control by a single slow mode, so that our quantitative treatment could be directly applied to the experimental data.

Summarizing this section, it is possible to conclude that the relaxational control over ET is expected when the slow reorganization energy Λ is comparable with or greater than $-\Delta G^0$. Two different types of kinetic behavior could be expected, namely: an oscillating ET (that could occur in a picosecond time scale), or a monotonically relaxing ET. On a longer time scale, the ET kinetics can be approximated, generally, by two components. The faster component reflects the nonadiabatic ET. The slower component is due to the relaxation; this component may reveal a complex dynamic behavior. It is noteworthy that the relative extents of two components are predicted to be sensitive to the changes in ΔG^0 of the ET reaction. This feature allows discrimination of the kinetic heterogeneity due to the relaxation control over ET from those due to other reasons (see above).

Low-exothermic ET reactions in the bacterial photosynthetic reaction center

As follows from the previous section, one has to know the value of the slow reorganization energy Λ to decide whether an ET reaction with a given ΔG^0 is relaxationally controlled. To find out the value of Λ for protein-mediated ET reactions, we used the experimental data on ET in the photosynthetic reaction centers (RC) of purple phototrophic bacteria *Rhodopseudomonas viridis* and *Rhodobacter sphaeroides*. RCs are pigment–protein complexes that catalyze the conversion of light energy into chemical energy (see Parson, 1991; Lancaster and Michel, 1997 for reviews). The crystal structures, resolved for the RC from *Rhodopseudomonas viridis* (Deisenhofer et al., 1984) and from *Rhodobacter sphaeroides* (Allen et al., 1987), show a core that is formed by the integral membrane L and M subunits and that is capped by the H subunit from the cytoplasmic side of the membrane (see Fig. 2 *A* for the x-ray structure of the *Rps. viridis* RC). In the case of *Rps. viridis*, a tetraheme cytochrome *c* is attached from the periplasmic side as depicted in Fig. 2 *A*. In the case of *Rb. sphaeroides*, the bound cytochrome subunit is absent, and a water-soluble cytochrome *c* serves as a mobile electron donor for the RC. As shown schematically in Fig. 2 *A*, the photoexcitation of the bacteriochlorophyll dimer *P* is followed by a picosecond electron transfer across the membrane, via a monomeric bacteriochlorophyll B_A and a bacteriopheophytin H_A, to a bound primary ubiquinone Q_A (menaquinone MQ_A in *Rps. viridis*). After that, the electron goes to a loosely bound secondary ubiquinone Q_B and reduces it to the semiubiquinone anion Q_B^-. The reduction of Q_B^- by the next electron leads to the proton trapping from the medium and to the formation of an ubiquinol Q_BH_2 at ~100 μs. The oxidized P^+ is reduced by a *c*-type cytochrome. In the case of the tetraheme cytochrome *c* of *Rps. viridis* (see Fig. 2 *A*), the nearest heme serves as an immediate electron donor and is later re-reduced by the remote hemes (Dracheva et al., 1988). Generally, the time constant of P^+ reduction varies between 100 ns and 100 μs depending on the bacterial species.

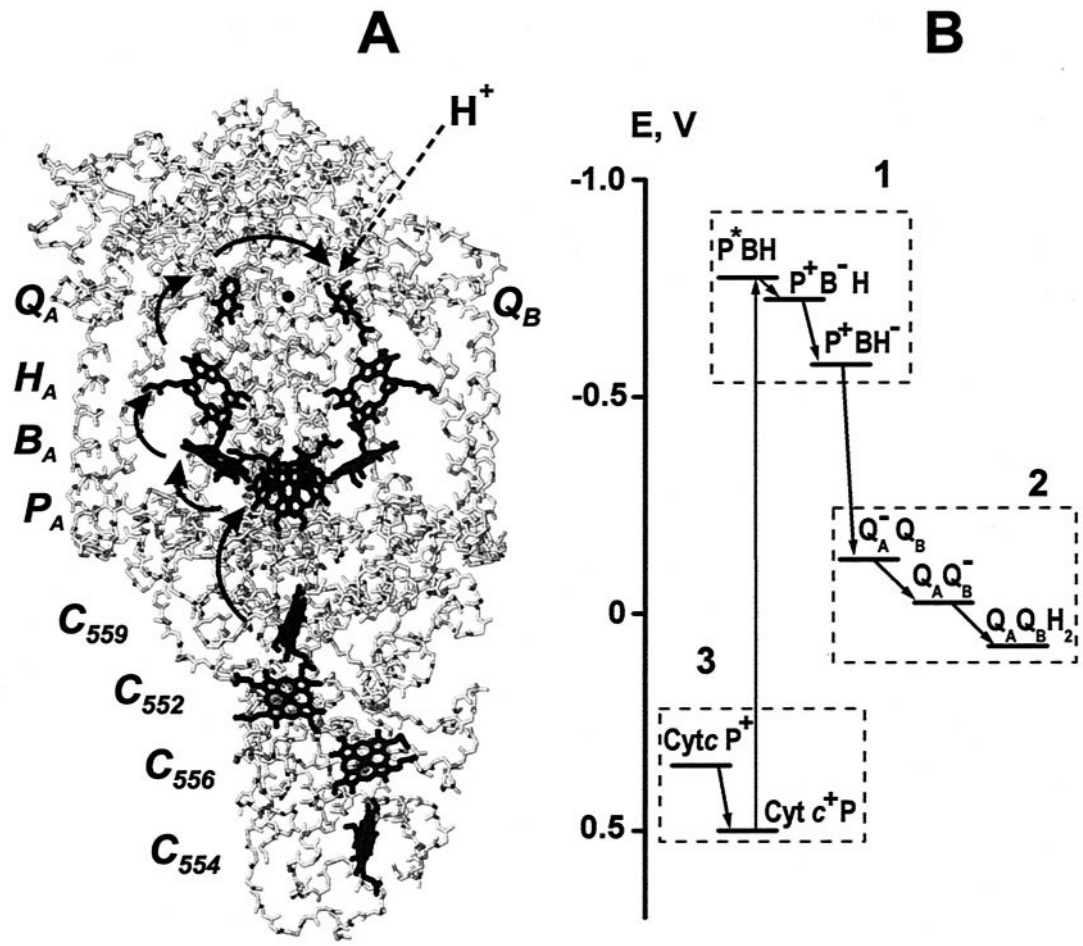

FIGURE 2 Bacterial photosynthetic reaction center. (*A*) The x-ray structure of the bacterial photosynthetic RC of *Rhodopseudomonas viridis* (Lancaster and Michel, 1997; 2PRC PDB entry was used). Redox cofactors are highlighted; solid arrows indicate the ET steps; the dashed arrow depicts the putative proton transfer route (see Lancaster and Michel, 1997, for further details). (*B*) Generalized energy level diagram of a bacterial RC (see Parson, 1991, for review and the text for further references). The bars account for the variation of the experimentally determined redox potential values between the best studied RC of *Rhodobacter sphaeroides* and *Rps. viridis.*

The possibility to trigger a single RC turnover by a short laser flash and to monitor the subsequent redox changes of the cofactors has prompted a vast number of experimental ET studies (see Moser et al., 1992; Okamura et al., 2000; Gunner and Alexov, 2000 for reviews). In many cases, ET reactions have been characterized to an extent that allows categorization of their kinetic components as nonadiabatic or relaxational ones, respectively. Figure 2 *B* shows a generalized energy level diagram of a bacterial RC. The dashed boxes mark the low-exothermic ET steps for which a relaxational control could be expected. Hereafter we consider these steps one by one.

Oscillatory features in the primary charge separation

An oscillating ET (see the previous section) could be expected only for the primary charge separation reactions (see box #1 in Fig. 2). A number of oscillating phenomena coupled with these reactions has been observed (see Vos and Martin, 1999, for review). The mechanism of the observable oscillations and their role in the primary ET reactions are still unclear (see discussion in Lucke et al., 1997; Spörlein et al., 1998). In several particular cases, synchronized out-of-phase oscillations of the populations of the excited state P^*B_A and the charge separated state $P^+B_A^-$, apparently coupled with ET, have been reported (Streltsov et al., 1997, 1998; Yakovlev et al., 2000). A coherent vibration in the formation of the $P^+H_A^-$ dipole with a frequency of 30 cm^{-1} has been monitored by the electrochromic shift of the B_A absorption (Vos et al., 2000). All these oscillations can hardly be attributed to quantum effects (see Lucke et al., 1997; Bixon and Jortner, 1997a, 1997b for the theory of quantum coherence in ET), because energetically comparable quantum oscillations with frequency of ~30 cm^{-1} should be effectively de-phased at room temperature by thermal motion and intrastate relax-

ation. The molecular dynamics simulations of the RC, from the other side, revealed several classical vibrational modes with frequencies of 20–100 cm^{-1} altering the electrostatic energy gap of the $P^*B_A \rightarrow P^+B_A^-$ ET reaction (Parson et al., 1998a). The latter modes could directly relate to the low-frequency underdamped relaxation in Eq. 14.

In Fig. 3, we replotted (from Yakovlev et al., 2000) the experimental data on the oscillations of the $P^+B_A^-$ state in the RCs of *Rb. sphaeroides* where the bacteriopheophytin *a* has been replaced by pheophytin *a*. From these data taken at face value, it follows that the rate constant of the intrinsic electron delivery to B_A is $\geq 5 \cdot 10^{12}$ s^{-1} and that the reduction of B_A is modulated by an oscillating mode (Q_1) with period of ~250 fs, and by a slower relaxation mode (Q_2) with characteristic time of ~1.5 ps. We applied the Langevin stochastic approach to analyze this data set. On modeling, we assumed that the ET reaction is adiabatic and can be described by Eq. 2. Then the probabilities of precursor (P^*B_A) and product ($P^+B_A^-$) states, $P_A(t)$ and $P_B(t)$, respectively, obey the kinetic Eqs. 11 with the rate constants k_{AB} and k_{BA} as determined by Eqs. 10 and 9. The dynamics of the oscillation coordinate Q_1 and of the relaxation coordinate Q_2 were described by two stochastic equations, 14.

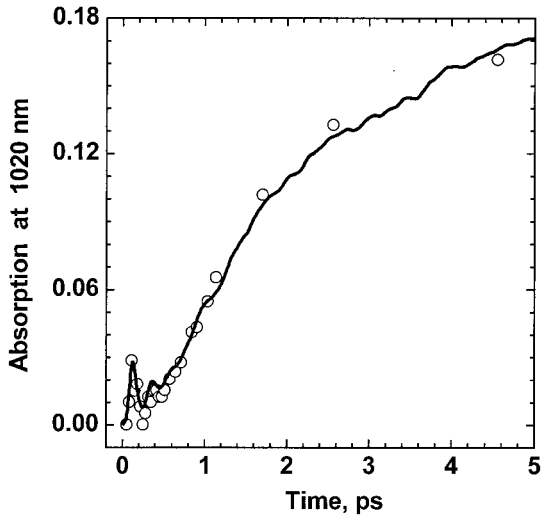

FIGURE 3 Kinetics of bacteriochlorophyl B_A reduction in the pheophytin-*a* substituted RCs of *Rb. sphaeroides* (the experimental points were re-plotted from Yakovlev et al. (2000). The solid curve was obtained by numeric integration of the two stochastic differential Eq. 14 in combination with the kinetic Eqs. 11; an ensemble of 100 random trajectories was averaged to achieve a reliable sampling of the stochastic dynamics. The solution was obtained by a numeric integration using the modified Runge–Kutta algorithm (Brankin et al., 1992). The following parameter values were used: $\Delta G^0 = -20$ meV (in accordance with Yakovlev et al., 2000; $\lambda = 40$ meV, $\Lambda_1 = 58$ meV, $\Lambda_2 = 41$ meV (the total reorganization energy of ~120 meV was calculated for the time interval of 2 ps both by molecular dynamics (Parson et al., 1998b) and by continuum electrostatics (Krishtalik, 1995)); $\omega_{eff} = 400$ cm^{-1}, $\Omega_1 = 150$ cm^{-1}, $\Omega_2 = 20$ cm^{-1} (both estimates were directly obtained from the kinetic trace), $\Gamma_1 = 25$ cm^{-1}, $\Gamma_2 = 10$ cm^{-1}, $Q_1(0) = -0.3$, $Q_2(0) = 0$.

The values of most model parameters were either taken from the literature or directly acquired from the modeled experimental data (the full list of variables and the respective references could be found in the caption to Fig. 3). Two low-frequency modes with $\Omega_1 = 150$ cm^{-1}, $\Lambda_1 = 58$ meV, and $\Omega_2 = 20$ cm^{-1}, $\Lambda_2 = 41$ meV were needed to fit the experimental data (see caption to Fig. 3 for other fit parameters). The minor random oscillations of the fit curve at $t >$ 0.5 ps reflect the residual noise after averaging of 100 independent solutions of the stochastic Langevin equation.

Although the results are at best illustrative, the modeling showed that the oscillating features in the B_A reduction kinetics can be quantified in the terms of relaxationally controlled ET. In our hands, the amplitude of the modeled oscillations was very sensitive to the relationship between Λ_1, Λ_2, and ΔG^0, whereas the values of other parameters were less significant for the ET dynamics. This sensitivity might explain why the oscillating ET features are less pronounced in the nonmodified, native RC (Spörlein et al., 1998; Vos et al., 2000): the pheophytin *a* reconstitution could disturb the RC structure and thereby might increase the reorganization energy of $P^+B_A^-$ formation or decrease the free energy gap between P^*B_A and $P^+B_A^-$ states.

Ubiquinone reactions: $Q_A^-Q_B \rightarrow Q_AQ_B^-$ *electron transfer*

The ET reactions of ubiquinone cofactors (see box #2 in Fig. 2 *B* and reaction I) are most comprehensively studied in the RC of *Rb. sphaeroides* (see Shinkarev et al., 1992; Okamura et al., 2000 for reviews). The delivery of the first electron to Q_B causes the formation of a kinetically stable semiquinone anion radical Q_B^-.

$$Q_AQ_B \xrightarrow{1st\ h\nu} Q_A^-Q_B \rightleftharpoons Q_AQ_B^-$$

SCHEME I

While Q_B can be easily exchanged for a ubiquinone from the membrane pool, Q_B^- is tightly bound (Mulkidjanian et al., 1986; McPherson et al., 1990). Although the semiquinone itself stays deprotonated, its negative charge shifts the pK values of some amino acid residues in the vicinity and causes proton binding from the bulk, both in the case of the isolated RC (Wraight, 1979; Maroti and Wraight, 1988; McPherson et al., 1988) and of chromatophores (Gopta et al., 1999). The reaction shown in Scheme I could be monitored either by electron transfer (see e.g., Li et al., 1998) or by monitoring the changes in the transmembrane electric potential ($\Delta\psi$) caused by proton transfer from the surface into the Q_B site (Drachev et al., 1990; Brzezinski et al., 1997; Gopta et al., 1999).

In the isolated RC preparations, the free energy of the $Q_A^-Q_B \rightarrow Q_AQ_B^-$ reaction, $\Delta G_{AB}^{(1)}$, has been estimated as −60

meV (Li et al., 1998). In these preparations, the kinetics of Q_B reduction was apparently contributed by two components: a slow one k_s ($3–5 \cdot 10^3$ s^{-1}) with an activation energy E_a of ~400 meV, and a fast one k_f ($2–3 \cdot 10^4$ s^{-1}) with a smaller E_a of ~170 meV (Tiede et al., 1996, 1998; Li et al., 1998). In native membrane vesicles (chromatophores) of *Rb. sphaeroides*, where the free energy gap is larger ($\Delta G^{(1)}_{AB} \sim -100$ meV (see e.g., Cherepanov et al., 2000), a third, very fast component k_{vf} ($2.5 \cdot 10^5$ s^{-1}) has been resolved (Tiede et al., 1998). A similar component ($k_{vf} \sim 3 \cdot 10^5$ s^{-1}, $E_a \sim 170$ meV) appeared gradually in the ET kinetics of isolated RC preparations when the free energy gap $\Delta G^{(1)}_{AB}$ was increased from −60 to −160 meV by replacing Q_A by its low-potential analogues (Li et al., 1998, 2000). The rate of the latter k_{vf} component has been shown to depend on $\Delta G^{(1)}_{AB}$ (Li et al., 2000).

From its dependence on $\Delta G^{(1)}_{AB}$, the k_{vf} component of the Q_B reduction has been identified as the initial, nonadiabatic ET (Okamura et al., 2000; Li et al., 2000). Correspondingly, the k_f and k_s components could be attributed to the relaxation (Cherepanov et al., 2000; Li et al., 2000). The independence of their rates of $\Delta G^{(1)}_{AB}$ (Graige et al., 1998; Li et al., 2000) supports this attribution.

We applied Eqs. 15, which connect the relative amplitudes of the fast, nonadiabatic component of ET with the equilibrium energy gap, ΔG^0, and the slow part of reorganization energy, Λ, to estimate Λ of the $Q_A^- Q_B \rightarrow Q_A Q_B^-$ reaction from the available experimental data. The values of $\Delta G^{(1)}_{AB}$ and of the relative contributions of the very fast component, A_{vf}, at room temperature were taken from the works cited above. The resulting values of Λ are presented in Table 1. They vary around 100 meV and correspond thus to the estimate of 90 meV that has been obtained recently, from analogous energy considerations, by Gunner and coworkers (Li et al., 2000). The latter authors have conceived a single relaxational reaction at ~100 μs that proceeds around either Q_A or Q_B (Li et al., 2000). In our opinion, the presence of two slower components in the ET kinetics, namely of k_f and k_s, could be better understood from at least two relaxation modes.

The fast k_f component correlates kinetically with the proton rearrangement in the Q_B^- binding cavity in response to the appearance of a negative charge (Gopta et al., 1999). These proton displacements are traceable both in the RCs and in native chromatophores via changes both in pH (Wraight, 1979; Gopta et al., 1999) and in the membrane potential, $\Delta\psi$, (Drachev et al., 1990; Gopta et al., 1997; Brzezinski et al., 1997). Such a protonic relaxation seems to serve as a prerequisite for ET from Q_A^- to Q_B (see Takahashi et al., 1992; Cherepanov et al., 2000, for more details) and might be accompanied by minor, low-barrier displacements of the ionizable protein groups (Gunner and Alexov, 2000).

The slower k_s component might be coupled with a major rotation of the Q_B ring. Earlier, it has been shown that the $Q_A^- Q_B \rightarrow Q_A Q_B^-$ reaction could be frozen in the dark-adapted RC, but not in the pre-illuminated ones (Berg et al., 1979; Kleinfeld et al., 1984). These observations have prompted the concept of the conformationally gated ET in the RC. The low-temperature x-ray structures of the *Rb. sphaeroides* RC (Stowell et al., 1997) provided an explanation for this freezing phenomenon: they have revealed that a large fraction of Q_B molecules is in a distal position relative to Q_A and has to move into the proximal one to be reduced to Q_B^-. (The position of Q_B^- is only 2 Å closer to Q_A than the distal Q_B position [Stowell et al., 1997]. The quinone ring stabilization is, however, quite different in these two positions: in the distal position, it is stabilized only by a single bond with Ile-L224, whereas Q_B^- is stabilized by five hydrogen bonds with His-L190, Ser-L223, Ile-L224, Gly-L225 and Thr-L226 (Stowell et al., 1997). Therefore, we believe that the absence of ET to Q_B in its distal position is rather due to a positive ΔG of the reaction [because of the limited possibility to stabilize Q_B^- in this position] than to the slightly larger distance.) As the displacement of Q_B into the proximal position is coupled with a rotation of the quinone ring by 180° (Stowell et al., 1997), it is likely that the k_s component of the Q_B reduction, with its relatively high E_a, is coupled with this conformational change (see Cherepanov et al., 2000, for further details).

The relative contributions of the faster, "protonic" and the slower, "conformational" modes to the total Λ could be estimated only roughly. The protonic relaxation is driven by the electrostatic interaction of Q_B^- with the surrounding ionizable residues. From the functional data, this interaction has been estimated as ≤85 mV (Shinkarev et al., 1992; Cherepanov et al., 2000). The residual contribution to Λ of

TABLE 1 Kinetic parameters of the low-exothermic ET steps in RCs of *Rhodobacter sphaeroides* and *Rhodopseudomonas viridis* (see text for details)

ET Reaction	ΔG^0 (meV)	k_{vf} (s^{-1})	A_{vf} (%)	Λ (meV)	Reference
Rhodobacter sphaeroides					
$Q_A^- Q_B \rightarrow Q_A Q_B^-$, chromatophores	−105	$2.5 \cdot 10^5$	60	95	Tiede et al., 1998
$MQ_A^- Q_B \rightarrow MQ_A Q_B^-$, menaquinone substituted RCs	−93	$3 \cdot 10^5$	40	103	Li et al., 1998
Rhodopseudomonas viridis, native RCs					
$P^+ c_{559} c^+_{556} c^+_{552} \rightarrow P c^+_{559} c^+_{556} c^+_{552}$	−112	$4.3 \cdot 10^6$	≤84	≥70	Ortega and Mathis, 1993
$P^+ c_{559} c_{556} c^+_{552} \rightarrow P c^+_{559} c_{556} c^+_{552}$	−122	$5.3 \cdot 10^6$	91	63	Ortega and Mathis, 1993
$P^+ c_{559} c_{556} c_{552} \rightarrow P c^+_{559} c_{556} c_{552}$	−180	$8.7 \cdot 10^6$	≥98	≤80	Ortega and Mathis, 1992

10–20 meV could then be attributed to the conformational displacement of Q_B. The latter estimate corroborates both with the relatively small and variable extent of k_s (Tiede et al., 1998; Li et al., 1998) and with the simultaneous observation of the proximal and distal Q_B populations in the RC structures (Stowell et al., 1997). Because the equilibrium between the two isoenergetic Q_B conformations is apparently controlled by the whole RC (Gopta et al., 1997; Mulkidjanian, 1999), the coupling of the slower relaxational mode to the ET proper is likely to be weak. The variations in this slow conformational mode, however, could account for the different A_{vf} values at the same ΔG, that have been observed when Q_A was replaced by naphtoquinones of different tail length (Li et al., 2000). The fine balance between the energies of the proximally and distally bound Q_B molecules might be well sensitive to the minor changes in the RC conformation induced by the differences in the Q_A tail length.

Ubiquinone reactions: $Q_A^-Q_B^- \rightarrow Q_AQ_BH^-$ transition

The delivery of the second electron to Q_B^- is tightly coupled with the binding of first proton and results in the formation of an ubiquinol anion Q_BH^- at ~100 μs. The second, separate protonation event (see Scheme II) yields a ubiquinol Q_BH_2 (see Okamura et al., 2000 for review).

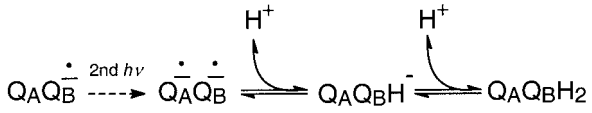

SCHEME II

The driving force of the first $Q_A^-Q_B^- + H^+ \rightarrow Q_AQ_BH^-$ step can be estimated as ~−100 meV at pH 7.0 (Takahashi and Wraight, 1992; Cherepanov et al., 2000). By analogy with the transfer of the first electron, a relaxational control over this reaction could be expected. Contrary to the expectation, the rate of this reaction depends on the free energy gap $\Delta G^{(2)}_{AB}$, as has been shown by using RC preparations with Q_A replaced by low-potential quinones (Graige et al., 1996). This finding has been interpreted as an evidence of a fast, non-rate-limiting protonation of a semiquinone anion ($Q_B^- + H^+ \rightarrow Q_BH^\cdot$) followed by a rate-limiting nonadiabatic ET reaction ($Q_BH^\cdot \rightarrow Q_BH^-$) (Graige et al., 1996; Okamura et al., 2000). The apparent absence of a notable relaxational control indicates that both conformational and protonic components of relaxation are minor in the time window of this ET reaction.

The absence of a significant conformational relaxation is not surprising, because both Q_B^- and the ubiquinol-anion Q_BH^- are likely to be fixed in similar positions (Lancaster and Michel, 1997). The absence of a notable protonic relaxation at hundreds of microseconds might be due to a low pK value of the $Q_B^-/Q_BH^\cdot$ couple. The rate of proton equilibration in the Q_B site is determined by the sum of proton binding and proton dissociation rate constants of the involved proton donors and proton acceptors. It has been recently shown that the same proton path, formed by acidic groups of Asp-L213, Asp-L210, and Asp-M17, is used to deliver protons to Q_B both on the first and on the second electron transfers (Paddock et al., 2000; Okamura et al., 2000). The nature of the proton accepting group(s), however, is quite different. On the first flash, the protons are accepted by some ionizable residues in the vicinity of Q_B; their pK values increase in response to the Q_B^- formation. At neutral pH, the apparent pK of the involved group(s) could be estimated as ~6.0 (Cherepanov et al., 2000), which corresponds to the time constant of protonic equilibration of ~50 μs (using the bimolecular rate constant of $2 \cdot 10^{10}$ $M^{-1}s^{-1}$ for protolytic reactions [Eigen, 1963]). This estimate is in good correspondence with the experimentally established time constant of the k_f component in the kinetics of the first electron transfer (Tiede et al., 1996, 1998; Li et al., 1998) and of the respective kinetic component of the electrogenic proton displacement (Gopta et al., 1997). In the particular case of the second electron transfer, the proton is trapped at any pH by Q_B^- itself. Because the pK of $Q_B^-/Q_BH^\cdot$ couple is less than 4.0 in the isolated RC (Lavergne et al., 1999), protons can equilibrate in less than 10^{-6} s. In this rather exceptional case, the protonic relaxation seems to contribute to the faster, nonadiabatic component of reorganization.

After the replacement of Asp-L213 by Asn, the rate of the $Q_A^-Q_B^- \rightarrow Q_AQ_BH^-$ reaction drastically slows down and becomes independent of $\Delta G^{(2)}_{AB}$ (Paddock et al., 1998). It has been concluded that the transfer of the second electron becomes limited by proton diffusion to Q_B^- in this mutant (Paddock et al., 1998; Okamura et al., 2000). According to an estimate from Cherepanov et al. (2000), the Asp-L213→Asn mutation slows the proton transfer to Q_B^- by three orders of magnitude. Thereby the proton relaxation control over the second electron transfer is imposed.

Cytochrome reactions: $P^+c_{599} \rightarrow Pc^+_{559}$

The reduction of the photo-oxidized P^+ by a *c*-type cytochrome is another low-exothermic ET reaction ($\Delta G_{cP} \sim -100$ meV) that could be controlled by relaxation (see box #3 in Fig. 2). The most comprehensive set of data has been collected for the RC of *Rps. viridis* shown in Fig. 2 *A* (Kaminskaya et al., 1990; Ortega and Mathis, 1992, 1993). Here the kinetics of the P^+ reduction by the nearest c_{559} heme contained a dominant very fast component ($k_{vf} \sim 5 \cdot 10^6$ s^{-1}) and a minor fast component ($k_f \sim 5 \cdot 10^5$ s^{-1}) at room temperature (Ortega and Mathis, 1992, 1993). The sequential reduction of other cytochrome *c* hemes caused a gradual increase in the energy gap between P^+ and c_{559}

because of the electrostatic impact of the additional negative charges (Gunner and Honig, 1991). This reduction was accompanied by an increase in k_{vf} from $4.3 \cdot 10^6$ (one heme pre-reduced) to $8.7 \cdot 10^6$ (three hemes pre-reduced) (Ortega and Mathis, 1992, 1993). At decreasing temperature, the relative contribution of k_{vf} dropped in favor of the slower kinetic components. The k_{vf} component, however, was not ousted completely, its contribution remained even below 100 K (Kaminskaya et al., 1990; Ortega and Mathis, 1992, 1993), i.e., under conditions where both the protonic and the conformational relaxation modes are expected to be essentially blocked. Hence, the k_{vf} component depended on ΔG_{cP} and on temperature in a way that allows one to attribute it to the nonadiabatic ET. Under this assumption, we estimated the values of Λ by applying Eqs. 15 to the experimental data on the relative amplitude of the k_{vf} component at different redox potentials (as acquired from Ortega and Mathis, 1992, 1993; see Table 1). The ΔG_{cP} value for the case with only c_{559} heme pre-reduced was derived from experimental data in Gao et al. (1990). The estimated changes in ΔG_{cP} in response to the reduction of c_{556} and c_{552} hemes were taken from Gunner and Honig (1991). As it follows from Table 1, the resulting Λ values of the ET reaction between the tetraheme cytochrome *c* (in different redox states) and P^+ seem to vary around 70 meV.

Summarizing, the low-exothermic ET reactions in the bacterial RCs seem to be essentially determined by the medium relaxation even in the time scale of hundreds of microseconds. With a single and explainable exception, the energies of the slow reorganization Λ, as obtained in this work, varied in the range of 70–100 meV. Rather minor modifications could switch the mechanism of ET between relaxational and nonadiabatic regimes. The increase in the driving force favored the nonadiabatic components in ET kinetics, whereas the slowing of the relaxation modes provoked the relaxational control over ET.

Outlook and implications for biological ET

The relaxation processes in proteins have very broad time distribution. Due to the constrained mobility of polar groups, different types of motion (orientational Debye-type polarization, frictional movement of charged residues, displacements of protein domains, etc.) occur in different time intervals from picoseconds to seconds (see e.g., Frauenfelder et al., 1991; Gunner and Alexov, 2000). Their contributions to the reorganization energy have been shown to be in the order of 50–200 meV even in the time scale of nanoseconds (Peloquin et al., 1994; Krishtalik, 1995; Cherepanov et al., 1998) and of microseconds (Shopes and Wraight, 1987; McMahon et al., 1998).

Protons are the only charged species that can move relatively free along water-filled protein cavities in response to a change in the charge state. An illustrative example of such a cavity has been found in the plant cytochrome *f* where a chain of water molecules, going through this elongated protein, connects the *c*-type heme with the protein surface (Martinez et al., 1996). Because of the long-range nature of electrostatic forces and of relatively low dielectric permittivity of proteins (Mertz and Krishtalik, 2000), the contribution of protonic relaxation could hardly be <50 meV. Its rate, generally, is determined by the rate constants of proton binding and dissociation. At neutral pH, the ionizable groups with neutral pK values are those usually involved; as a result, the protonic equilibration proceeds predominantly in the time scale of microseconds, provided that proton transfer is not mechanically hampered. We tend to separate the relatively slow proton diffusion from other types of proton motion (vibration and reorientation of covalent bonds, proton shifting along hydrogen bonds, etc.). One reason is that the latter, faster proton motions are the obligatory constituents of conformational relaxation. Another reason is the importance of the long-range proton diffusion for bioenergetic reactions: the mechanism of transmembrane proton transfer by redox-driven proton pumps represents, in its essence, a series of ET-coupled proton diffusion reactions. Here we tried to demonstrate that such proton relaxation reactions are indispensable to the low-exothermic ET. Nature had just to order them in time and space to yield proton pumps.

Thus, energetically comparable relaxation processes of different nature seem to accompany ET in proteins in a wide time range. The superposition of several relaxation modes with different characteristic times allows an understanding of why Λ remains in the order of 100 meV in the whole submillisecond time domain.

By varying the ΔG value of different ET reactions in the bacterial RC and by analyzing the experimental data on ET in other proteins, Dutton and colleagues have found that λ ranges usually between 0.7 and 1 eV in proteins (Gunner and Dutton, 1989; Moser et al., 1992). Correspondingly, the slow reorganization energy Λ comprises roughly one-tenth of the total reorganization energy of biological ET. Assuming, from considerations above, that Λ of $\sim$100 meV is typical for ET reactions in proteins that proceed in the submillisecond time scale, the relaxational control over nonadiabatic ET could be expected if ΔG of an ET reaction is ≥ -100 meV (see Eqs. 15). In a recently published survey (Page et al., 1999), the ET in 130 different redox proteins has been analyzed. From the predominantly short distances between the redox centers, it has been concluded that, in the vast majority of cases, the expected optimal ET rates (at $\lambda \sim -\Delta G^0$) are faster than 10^8 s^{-1}. It is noteworthy that for $\sim$90% of the surveyed reactions ΔG^0 was ≥ -100 meV (P. L. Dutton, personal communication). Because the proteins for the survey have been chosen just based on the availability of their x-ray structures, the fraction of low-exothermic reactions in the whole wealth of redox proteins is likely to be comparably high. The predominance of low-exothermic ET reactions compels us to expect the preva-

lence of the relaxational ET mechanism in biology. The relaxational control over ET might be a plausible reason why ET in proteins is often much slower than it could be predicted from the empirical equation relating the rate of nonadiabatic ET in proteins to distance (Moser et al., 1992).

In practice, the experimental discrimination between protonic and conformational relaxation modes could be facilitated by the notion that the former are likely to have a low E_a, but depend both on pH and on the H/D isotope substitution (at different pH, differently buried ionizable groups seem to be involved in the proton exchange, see Gopta et al., 1999). The conformational relaxation, in contrast, is likely to depend weakly on pH and on the H/D substitution, but could be remarkably temperature dependent. The reduction of the photo-oxidized primary donor of the photosystem II (P^+_{680}) by a redox-active tyrosine Y_Z can serve as an illustrative example. Here the ET kinetics contain a fast component of 20–50 ns (that has been attributed to the nonadiabatic ET [Karge et al., 1996]) and several slower relaxational components. The faster of them, with $\tau \sim 500$ ns, is independent both of pH and H/D substitution (Meyer et al., 1989; Karge et al., 1996; Haumann et al., 1997). It has been putatively attributed to a conformational relaxation (Cherepanov et al., 1998). This attribution is in agreement with the optoacoustic data on the photosystem II volume change in the time scale of hundreds of nanoseconds in response to the initial charge separation (Yruela et al., 1994). The slower relaxation at 1–30 μs is sensitive to the H/D substitution and has been, correspondingly, attributed to the protonic relaxation (Schilstra et al., 1998).

On studying the dependence of an ET reaction on various factors (such as pH, H/D substitution, mutations, temperature, etc.), it is rather useful to take into account that the observable changes in the ET rate might reflect the effect of those factors on the relaxation mode(s) and not on the nonadiabatic ET proper. In such cases, the classical theory of nonadiabatic ET can hardly be used to analyze the data. Instead, some quantitative treatment of a relaxationally controlled ET should be applied. It is noteworthy that, in many cases, the nature of the dominating relaxational mode can be identified with confidence (the gated ET reactions that are surveyed in Sharp and Chapman (1999) may serve as examples). Then the relaxation process proper could be studied through ET. In most cases, it is easier to monitor an ET reaction than, for example, protonic redistribution or a conformational change. The approach that we suggested here might help to extract quantitative information from this kind of data.

APPENDIX A: DESCRIPTION OF ET DYNAMICS IN TERMS OF SPECTRAL FUNCTION

The vibrational characteristics of reactants and polar solvent were approximated by thermally equilibrated linear oscillators as described in the text. We assumed that the complete information about the system is encapsulated in the single "spectral function" $J(\omega)$. The latter can be expressed through the complex dielectric permittivity of the solvent $\varepsilon(\omega)$ and the difference of dielectric displacements in the reactant and product states $\Delta\mathbf{D}(\mathbf{r}) = \mathbf{D}_B(\mathbf{r}) - \mathbf{D}_A(\mathbf{r})$ (see e.g., Ulstrup, 1979),

$$J(\omega) = \frac{1}{2}\sum_j m_j\omega_j^3\delta_j^2\delta(\omega - \omega_j)$$

$$= \frac{1}{4\pi^2}\cdot\frac{\operatorname{Im}\varepsilon(\omega)}{|\varepsilon(\omega)|^2}\cdot\int|\Delta\mathbf{D}(\mathbf{r})|^2\,d\mathbf{r}. \qquad (A.1)$$

The spectral function can also be represented as the Fourier transform of the energy–energy correlation function $C(t) = \langle\Delta E(t)\Delta E(0)\rangle$ where $\Delta E(t)$ is the energy gap between product and reactant states (Warshel et al., 1989),

$$J(\omega) = \frac{\pi\omega}{kT}\int_{-\infty}^{\infty}C(t)\exp(-i\omega t)\,dt. \qquad (A.2)$$

$J(\omega)$ can be found thereby either by means of continuum electrostatics or by the analysis of molecular dynamics trajectories. The reorganization energy could then be expressed as an integral of the spectral function (Xu and Schulten, 1994),

$$\lambda = \frac{1}{2}\sum_j m_j\omega_j^2\delta_j^2 = \int\frac{J(\omega)}{\omega}\,d\omega.$$

The spectral function of polar solvents includes several frequency intervals. The optical and highest infrared polarization modes (the frequency of 10^{15}–10^{14} s^{-1}) comprise the inertialess part of polarization and do not contribute to the reorganization energy. The intramolecular vibrations (10^{14}–10^{13} s^{-1}) are usually faster than the frequency of thermal fluctuations ($\approx 10^{13}$ s^{-1} at room temperature) and should be described by means of quantum mechanics. Slower intermolecular and orientational fluctuations in the range of 10^{12}–10^{10} s^{-1} could be treated at room temperature as classical. The effective frequency ω_{eff} of classical fluctuations,

$$\omega_{eff}^2 = \int_0^{kT/\hbar}\omega J(\omega)\,d\omega\int_0^{kT/\hbar}\omega^{-1}J(\omega)\,d\omega, \qquad (A.3)$$

determines the average rate of adiabatic ET (Kuznetsov, 1989),

$$k_{ad} = (2\pi)^{-1}\omega_{eff}\exp(-E_a/k_BT). \qquad (A.4)$$

The rate of nonadiabatic ET can be expressed through the spectral function using the theory of spin-boson Hamiltonian (see e.g., Leggett et al., 1987; Warshel et al., 1989)),

$$k_{na} = \left(\frac{V}{\hbar}\right)^2\int_{-\infty}^{\infty}\cos[(\Delta G^0\cdot s + W_1(s))/\hbar]\exp[-W_2(s)/\hbar]\,ds, \qquad (A.5)$$

where

$$W_1(s) = \int_0^{\infty}\frac{J(\omega)}{\omega^2}\sin(\omega s)\,d\omega, \qquad (A.6)$$

$$W_2(s) = \int_0^\infty \frac{J(\omega)(1 - \cos(\omega s))}{\omega^2} \coth(\hbar\omega/2k_BT)\, d\omega. \quad (A.7)$$

Equations A.5–A.7 were derived by a complete quantum consideration and are valid for all temperature values. The overall rate constant of electron transfer is controlled by the slowest reaction and can be approximated by the equation (see e.g., Rips and Jortner, 1987a)

$$k_{ET} = \frac{k_{na}k_{ad}}{k_{na} + k_{ad}}. \quad (A.8)$$

The rate constant k_{ET} determines the characteristic time that separates the fast and slow nuclear motions in the system.

The application of Eqs. A.5–A.7 is complicated by the necessity of defining the spectral function and calculating the double integrals. In the high-temperature limit, where the thermal fluctuations are faster than all modes coupled to ET, Eq. A.5 could be simplified. In this case, $\hbar\omega/2kT$ and ωs are <1, so that functions A.6–A.7 read

$$W_1(s) = \lambda s, \quad (A.9)$$

$$W_2(s) = \lambda k_B T s^2. \quad (A.10)$$

The resulting integral,

$$k_{na} = \left(\frac{V}{\hbar}\right)^2 \int_{-\infty}^{\infty} \cos[(\Delta G^0 \cdot s + \lambda s)/\hbar]\exp[-\lambda k_B T s^2/\hbar]\, ds, \quad (A.11)$$

reproduces the Marcus equation,

$$k_{na} = \frac{2\pi}{\sqrt{4\pi\lambda k_B T}} \left(\frac{V}{\hbar}\right)^2 \exp\left(-\frac{(\lambda + \Delta G^0)^2}{4\lambda k_B T}\right). \quad (A.12)$$

The spectral function enters into Eq. A.12 only through the reorganization energy λ.

At the long time scale, the energy gap between precursor and product states depends on the value of slow coordinates Q_j. The dependence could be found by averaging the energy difference in the configuration space of the coordinates q_j,

$$\Delta G\{Q_j\} = \Delta G^0 + \Lambda - \sum_j M_j\Omega_j^2\Delta_j Q_j. \quad (A.13)$$

The activation energy in Eq. A.12 therefore depends on the slow coordinates,

$$E_a\{Q_j\} = \frac{1}{4}\lambda\left[1 + \frac{\Delta G^0}{\lambda} + \frac{1}{2\lambda}\sum_j M_j\Omega_j^2\Delta_j^2\left(1 - 2\frac{Q_j}{\Delta_j}\right)\right]^2. \quad (A.14)$$

APPENDIX B: LANGEVIN STOCHASTIC APPROACH TO THE ET DYNAMICS IN THE EFFECTIVE POTENTIAL

We described the dynamics of the slow coordinates Q_j in terms of the stochastic differential equations by using the Langevin approach. The basic stochastic equation of motion in potential $U(Q)$ is

$$M\frac{d^2Q}{dt^2} + M\cdot\Gamma\frac{dQ}{dt} + \frac{\partial U}{\partial Q} = (2M\Gamma k_B T)^{1/2}F(t), \quad (B.1)$$

where M is the effective mass, Γ is the damping factor, and $F(t)$ is the random force. In accordance with the fluctuation–dissipation theorem, $F(t)$ satisfies the conditions $\langle F(t)\rangle = 0$, $\langle F(t_1)F(t_2)\rangle = \delta(t_1 - t_2)$.

In our case, the relaxational dynamics of the slowly changing coordinates Q_j are determined by the decrease of free energy in accordance with the second law of thermodynamics. Such kind of dynamics could be quantified by the method of effective potential (see e.g., Landau and Lifshitz, 1959). The microscopic state of the system is thereby represented by a point moving along a stochastic trajectory $\{Q_j(t)\}$ on the multidimensional surface of the effective potential $U\{Q_j\}$. The usage of the effective potential implies a fast thermal equilibrium in the configuration space of the fast coordinates q_j at any given configuration of the slow coordinates Q_j. In our case, the fast configuration space also includes, besides the coordinates q_j, two electronic states, A and B. In the equilibrium, the distribution function $P\{q, Q\}$ obeys the Boltzmann statistical distribution,

$$P\{q, Q\} = \exp\left(-\frac{U_A\{q, Q\}}{k_B T}\right) + \exp\left(-\frac{U_B\{q, Q\}}{k_B T}\right), \quad (B.2)$$

where the respective potential energies $U_A\{q, Q\}$ and $U_B\{q, Q\}$ are defined by Eqs. 7. The effective potential $U\{Q\}$ is defined through the partial distribution function,

$$P\{Q\} = \int P\{q_i, Q\}\prod_i dq_i = \exp\left(-\frac{U\{Q\}}{k_B T}\right). \quad (B.3)$$

$U\{Q\}$ can be written as

$$U\{Q\} = -k_B T \ln\left[\int_{-\infty}^{\infty}\exp\left(-\frac{U_A\{q_i, Q\}}{k_B T}\right)\prod_i dq_i + \int_{-\infty}^{\infty}\exp\left(-\frac{U_B\{q_i, Q\}}{k_B T}\right)\prod_i dq_i\right]. \quad (B.4)$$

Because the potential energy is a square function of the coordinates, the integration can be done straightforwardly. Omitting the constant terms, we obtain

$$U\{Q\} = -k_B T \ln\left[\exp\left(-\sum_j \frac{M_j\Omega_j^2 Q_j^2}{2k_B T}\right) + \exp\left(-\sum_j \frac{M_j\Omega_j^2(Q_j - \Delta_j)^2 + \Delta G^0}{2k_B T}\right)\right]. \quad (B.5)$$

The first derivatives of $U\{Q\}$ read

$$\frac{\partial U}{\partial Q_j} = M_j\Omega_j^2 \frac{Q_j\exp(\mathcal{A}) + (Q_j - \Delta_j)\exp(\mathcal{B})}{\exp(\mathcal{A}) + \exp(\mathcal{B})}, \quad (B.6)$$

where

$$\mathcal{A} = -\sum_j \frac{M_j\Omega_j^2 Q_j^2}{2k_B T},$$

$$\mathcal{B} = -\sum_j \frac{M_j\Omega_j^2(Q_j - \Delta_j)^2 + \Delta G^0}{2k_B T}.$$

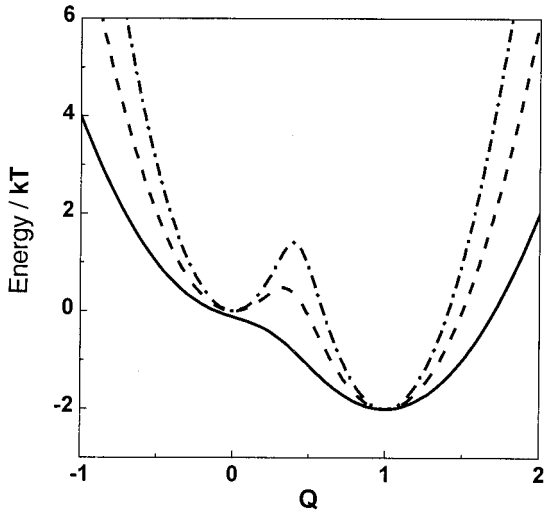

FIGURE 4 One-dimensional profile of $U(Q)$ for $\Delta G^0 = -2k_BT$. The curves were calculated by Eq. B.5 for $\Lambda = 4k_BT$ (*the lower line*), $\Lambda = 8k_BT$ (*the middle line*), and $\Lambda = 12k_BT$ (*the upper line*).

The exponential terms in this equation are just the Boltzmann probabilities $\bar{P}_A$ and $\bar{P}_B$ to find the system in the electronic states A and B, respectively,

$$\bar{P}_A\{Q\} = N_0^{-1}\exp\left(-\sum_j \frac{M_j\Omega_j^2Q_j^2}{2k_BT}\right), \quad (B.7)$$

$$\bar{P}_B\{Q\} = N_0^{-1}\exp\left(-\sum_j \frac{M_j\Omega_j^2(Q_j-\Delta_j)^2 + \Delta G^0}{2k_BT}\right), \quad (B.8)$$

where the normalizing constant N_0 is

$$N_0 = \exp\left(-\sum_j \frac{M_j\Omega_j^2Q_j^2}{2k_BT}\right) + \exp\left(-\sum_j \frac{M_j\Omega_j^2(Q_j-\Delta_j)^2 + \Delta G^0}{2k_BT}\right). \quad (B.9)$$

Generally, the effective potential that is described by Eq. B.5 has a two-well form. Figure 4 illustrates how the height of the barrier between two wells depends on the value of the slow reorganization energy Λ. When Λ becomes larger than the energy gap ΔG^0, the profile of $U(Q)$ changes gradually from a single-well to a double-well, which results in a localization of electron at one of the reactants.

Very helpful discussions with Drs. Leslie Dutton, Joshua Jortner, Marylin Gunner, Alexander M. Kuznetsov, Holger Lill, Mark Paddock, Vladimir A. Shuvalov, and Hans-Wilhelm Trissl are greatly appreciated. We thank Prof. Wolfgang Junge for his stimulating interest to this work and generous support.

This work has been supported in part by the Alexander von Humboldt Foundation and by grants from the Deutsche Forschungsgemeinschaft (Mu-1285/1, Ju-97/13), the Russian Foundation for Basic Research (99-04-48652), and INTAS (93-2852).

REFERENCES

Alexandrov, I. V. 1980. Physical aspects of charge transfer theory. *Chem. Phys.* 51:449–457.

Allen, J. P., G. Feher, T. O. Yeates, H. Komiya, and D. C. Rees. 1987. Structure of the reaction center from *Rhodopseudomonas viridis* R-26: the cofactors. *Proc. Natl. Acad. Sci. USA.* 84:5730–5734.

Bagchi, B., and N. Gayathri. 1999. Interplay between ultrafast polar solvation and vibrational dynamics in electron transfer reactions: role of high-frequency vibrational modes. *In* Electron Transfer—From Isolated Molecules to Biomolecules. J. Jortner and M. Bixon, editors. John Wiley & Sons, New York. 1–80.

Barbara, P. F., G. C. Walker, and T. P. Smith. 1992. Vibrational modes and the dynamic solvent effect in electron and proton transfer. *Science.* 256:975–981.

Berg, A. I., P. P. Noks, A. A. Kononenko, E. N. Frolov, and N. I. Uspenskaia. 1979. Conformational mobility and functional activity of photosynthetic reaction centers of *Rhodopseudomonas sphaeroides. Mol. Biol. (Mosk).* 13:469–477.

Bixon, M., and J. Jortner. 1997a. Vibrational coherence in nonadiabatic dynamics. *J. Chem. Phys.* 107:1470–1482.

Bixon, M., and J. Jortner. 1997b. Electron transfer via bridges. *J. Chem. Phys.* 107:5154–5170.

Bixon, M., and J. Jortner. 1999. Electron transfer—from isolated molecules to biomolecules. *In* Electron Transfer—From Isolated Molecules to Biomolecules. J. Jortner and M. Bixon, editors. John Wiley & Sons, New York. 35–202.

Brankin, R. W., I. Gladwell, and L. F. Shampine. 1992. RKSUITE: a suite of Runge–Kutta codes for the initial value problem for ODEs. Softreport 92-S1, Department of Mathematics, Southern Methodist University, Dallas, Texas.

Brzezinski, P., M. L. Paddock, M. Y. Okamura, and G. Feher. 1997. Light-induced electrogenic events associated with proton uptake upon forming Q_B^- in bacterial wild-type and mutant reaction centers. *Biochim. Biophys. Acta.* 1321:149–156.

Calef, D. F., and P. G. Wolynes. 1983. Smoluchowski–Vlasov theory of charge solvation dynamics. *J. Chem. Phys.* 78:4145–4153.

Cherepanov, D. A., S. I. Bibikov, D. A. Bloch, O. A. Gopta, D. Oesterhelt, A. Y. Semenov, and A. Y. Mulkidjanian. 2000. Reduction and protonation of the secondary quinone acceptor of *Rhodobacter sphaeroides* photosynthetic reaction center: kinetic model based on a comparison of wild type chromatophores with mutants carrying Arg→Ile substitution at sites 207 and 217 in the L-subunit. *Biochim. Biophys. Acta.* 1459: 10–34.

Cherepanov, D. A., W. Drevenstedt, L. I. Krishtalik, A. Mulkidjanian, and W. Junge. 1998. Protein relaxation and kinetics of P_{680}^+ reduction in photosystem II. *In* Photosynthesis: Mechanism and Effects. G. Garab, editor. Kluwer Academic Publishers, Dordrecht, The Netherlands. 1073–1076.

Crofts, A. R., S. Hong, N. Ugulava, B. Barquera, R. Gennis, M. Guergova-Kuras, and E. A. Berry. 1999. Pathways for proton release during ubihydroquinone oxidation by the bc_1 complex. *Proc. Natl. Acad. Sci. USA.* 96:10021–10026.

Deisenhofer, J., O. Epp, K. Miki, R. Huber, and H. Michel. 1984. X-ray structure analysis of a membrane complex: electron density map at 3 Å resolution and a model of the chromophores of the photosynthetic reaction center from *Rhodopseudomonas viridis. J. Mol. Biol.* 180: 385–398.

Dogonadze, R. R., and Z. D. Urushadze. 1971. Semiclassical method of calculation of chemical reactions proceeding in polar liquids. *J. Electroanal. Chem.* 32:234–245.

Drachev, L. A., M. D. Mamedov, A. Y. Mulkidjanian, A. Y. Semenov, V. P. Shinkarev, and M. I. Verkhovsky. 1990. Electrogenesis associated with proton transfer in the reaction center protein of purple bacteria *Rhodobacter sphaeroides. FEBS Lett.* 259:324–326.

Dracheva, S. M., L. A. Drachev, A. A. Konstantinov, A. Y. Semenov, V. P. Skulachev, A. M. Arutyunyan, V. A. Shuvalov, and S. M. Zaberezhnaya. 1988. Electrogenic steps in the redox reactions catalyzed by the photo-

synthetic reaction-center complex from *Rhodopseudomonas viridis*. *Eur. J. Biochem.* 171:253–264.

Eigen, M. 1963. Protonenübertragung, Säure-Base-Katalyse and enzymatische Hydrolyse. Teil I: Elementarvorgänge. *Angew. Chem.* 75: 489–588.

Frauenfelder, H., S. G. Sligar, and P. G. Wolynes. 1991. The energy landscapes and motions of proteins. *Science.* 254:1598–1603.

Gao, J. L., R. J. Shopes, and C. A. Wraight. 1990. Charge recombination between the oxidized high-potential *c*-type cytochromes and Q_A^- in reaction centers from *Rhodopseudomonas viridis*. *Biochim. Biophys. Acta.* 1015:96–108.

Garg, A., J. N. Onuchic, and V. Ambegaokar. 1985. Effect of friction on electron transfer in biomolecules. *J. Chem. Phys.* 83:4491–4503.

Gonzalez, M. A., E. Enciso, F. J. Bermejo, M. Jimenez-Ruiz, and M. Bee. 2000. Molecular approach to the interpretation of the dielectric relaxation spectrum of a molecular glass former. *Phys. Rev. E.* 61: 3884–3895.

Gopta, O. A., D. A. Bloch, D. A. Cherepanov, and A. Y. Mulkidjanian. 1997. Temperature dependence of the electrogenic reaction in the Q_B site of the *Rhodobacter sphaeroides* photosynthetic reaction center: the $Q_A^-Q_B \rightarrow Q_AQ_B^-$ transition. *FEBS Lett.* 412:490–494.

Gopta, O. A., D. A. Cherepanov, W. Junge, and A. Y. Mulkidjanian. 1999. Proton transfer from the bulk to the bound ubiquinone Q_B of the reaction center in chromatophores of *Rhodobacter sphaeroides*: retarded conveyance by neutral water. *Proc. Natl. Acad. Sci. USA.* 96:13159–13164.

Graige, M. S., G. Feher, and M. Y. Okamura. 1998. Conformational gating of the electron transfer reaction $Q_A^-Q_B \rightarrow Q_AQ_B^-$ in bacterial reaction centers of *Rhodobacter sphaeroides* determined by a driving force assay. *Proc. Natl. Acad. Sci. USA.* 95:11679–11684.

Graige, M. S., M. L. Paddock, J. M. Bruce, G. Feher, and M. Y. Okamura. 1996. Mechanism of proton-coupled electron transfer for quinone Q_B reduction in reaction centers of *Rb. sphaeroides*. *J. Am. Chem. Soc.* 118:9005–9016.

Gray, H. B., and J. R. Winkler. 1996. Electron transfer in proteins. *Ann. Rev. Biochem.* 65:537–561.

Gunner, M. R., and E. Alexov. 2000. A pragmatic approach to structure based calculation of coupled proton and electron transfer in proteins. *Biochim. Biophys. Acta.* 1458:63–87.

Gunner, M. R., and P. L. Dutton. 1989. Temperature and ΔG^0 dependence of the electron-transfer from BPh^- to Q_A in reaction center protein from *Rhodobacter sphaeroides* with different quinones as Q_A. *J. Am. Chem. Soc.* 111:3400–3412.

Gunner, M. R., and B. Honig. 1991. Electrostatic control of midpoint potentials in the cytochrome subunit of the *Rhodopseudomonas viridis* reaction center. *Proc. Natl. Acad. Sci. USA.* 88:9151–9155.

Hasted, J. B. 1973. Aqueous dielectrics. Chapman and Hall, London.

Haumann, M., O. Bögershausen, D. A. Cherepanov, R. Ahlbrink, and W. Junge. 1997. Photosynthetic oxygen evolution: H/D isotope effects and the coupling between electron and proton transfer during the redox reactions at the oxidizing side of photosystem II. *Photosynth. Res.* 51:193–208.

Hänggi, P., P. Talkner, and M. Borkovec. 1990. Reaction-field theory: fifty years after Kramers. *Rev. Mod. Phys.* 62:251–341.

Holzwarth, A. R., and M. G. Muller. 1996. Energetics and kinetics of radical pairs in reaction centers from *Rhodobacter sphaeroides*: a femtosecond transient absorption study. *Biochemistry.* 35:11820–11831.

Hynes, J. T. 1986. Outer-sphere electron-transfer reactions and frequency-dependent friction. *J. Phys. Chem.* 90:3701–3706.

Kaminskaya, O. P., A. A. Konstantinov, and V. A. Suvalov. 1990. Low temperature photooxidation of cytochrome *c* in reaction center complexes from *Rps. viridis*. *Biochim. Biophys. Acta.* 1016:153–164.

Karge, M., K. D. Irrgang, S. Sellin, R. Feinaeugle, B. Liu, H. J. Eckert, H. J. Eichler, and G. Renger. 1996. Effects of hydrogen/deuterium exchange on photosynthetic water cleavage in PS II core complexes from spinach. *FEBS Lett.* 378:140–144.

Kleinfeld, D., M. Y. Okamura, and G. Feher. 1984. Electron-transfer kinetics in photosynthetic reaction centers cooled to cryogenic temperatures in the charge-separated state: evidence for light-induced structural changes. *Biochemistry.* 23:5780–5786.

Kotelnikov, A. I., V. R. Vogel, A. V. Pastuchov, V. L. Voskoboinikov, and E. S. Medvedev. 1998. Coupling of electron transfer and protein dynamics. *In* Biological Electron Transfer Chains: Genetic, Composition and Mode of Operation. G. V. Canters and E. Vijgenboom, editors. Kluwer Academic Publishers, Dordrecht, The Netherlands. 29–51.

Krishtalik, L. I. 1995. Fast electron transfers in photosynthetic reaction centre: effect of the time-evolution of dielectric response. *Biochim. Biophys. Acta.* 1228:58–66.

Kuznetsov, A. M. 1989. Recent advances in the theory of charge transfer. J. O. Bockris, editor. Plenum Press, New York. 95–176.

Lancaster, C. R. D., and H. Michel. 1997. The coupling of light-induced electron transfer and proton uptake as derived from crystal structures of reaction centres from *Rhodopseudomonas viridis* modified at the binding site of the secondary quinone, Q_B. *Structure.* 5:1–22.

Landau, L., and E. M. Lifshitz. 1959. Statistical Physics. Pergamon Press, London, Paris.

Lavergne, J., C. Matthews, and N. Ginet. 1999. Electron and proton transfer on the acceptor side of the reaction center in chromatophores of *Rhodobacter capsulatus*: evidence for direct protonation of the semiquinone state of Q_B. *Biochemistry.* 38:4542–4552.

Leggett, A. J., S. Chakravarty, A. T. Dosey, M. P. A. Fisher, A. Garg, and W. Zwerger. 1987. Dynamics of the dissipative two-state system. *Rev. Mod. Phys.* 59:1–85.

Levich, V. G., and R. R. Dogonadze. 1959. The theory of nonradiative electronic transitions between ions in solutions. *Dokl. Akad. Nauk SSSR Ser. Fiz. Khim.* 124:123–126.

Li, J., E. Takahashi, and M. R. Gunner. 2000. ΔG^0 and pH dependence of the electron transfer from $P^+Q_A^-Q_B$ to $P^+Q_AQ_B^-$ in *Rhodobacter sphaeroides* reaction centers. *Biochemistry.* 39:7445–7454.

Li, J. L., D. Gilroy, D. M. Tiede, and M. R. Gunner. 1998. Kinetic phases in the electron transfer from $P^+Q_A^-Q_B$ to $P^+Q_AQ_B^-$ and the associated processes in *Rhodobacter sphaeroides* R-26 reaction centers. *Biochemistry.* 37:2818–2829.

Liebl, U., G. Lipowski, M. Negrerie, J. C. Lambry, J. L. Martin, and M. H. Vos. 1999. Coherent reaction dynamics in a bacterial cytochrome *c* oxidase. *Nature.* 401:181–184.

Loffler, G., H. Schreiber, and O. Steinhauser. 1997. Calculation of the dielectric properties of a protein and its solvent: theory and a case study. *J. Mol. Biol.* 270:520–534.

Lucke, A., C. H. Mak, R. Egger, J. Ankerhold, J. Stockburger, and H. Grabert. 1997. Is the direct observation of electronic coherence in electron transfer reactions possible? *J. Chem. Phys.* 107:8397–8408.

Marcus, R. A. 1956. On the theory of oxidation–reduction reactions involving electron transfer. I. *J. Chem. Phys.* 24:966–978.

Marcus, R. A. 1964. Chemical and electrochemical electron-transfer theory. *Ann. Rev. Phys. Chem.* 155–196.

Marcus, R. A., and N. Sutin. 1985. Electron transfers in chemistry and biology. *Biochim. Biophys. Acta.* 811:265–322.

Maroti, P., and C. A. Wraight. 1988. Flash-induced H^+-binding by bacterial photosynthesis reaction centers: influences of the redox states of the acceptor quinones and primary donor. *Biochim. Biophys. Acta.* 934: 329–347.

Martinez, S. E., D. Huang, M. Ponomarev, W. A. Cramer, and J. L. Smith. 1996. The heme redox center of chloroplast cytochrome *f* is linked to a buried five-water chain. *Protein Sci.* 5:1081–1092.

McMahon, B. H., J. D. Muller, C. A. Wraight, and G. U. Nienhaus. 1998. Electron transfer and protein dynamics in the photosynthetic reaction center. *Biophys. J.* 74:2567–2587.

McPherson, P. H., M. Y. Okamura, and G. Feher. 1988. Light-induced proton uptake by photosynthetic reaction centers from *Rhodobacter sphaeroides* R-26. I. Protonation of the one-electron states $D^+Q_A^-$, DQ_A^-, $D^+Q_AQ_B^-$, and $DQ_AQ_B^-$. *Biochim. Biophys. Acta.* 934:348–368.

McPherson, P. H., M. Y. Okamura, and G. Feher. 1990. Electron transfer from the reaction center of *Rb. sphaeroides* to the quinone pool: doubly reduced Q_B leaves the reaction center. *Biochim. Biophys. Acta.* 1016: 289–292.

Mertz, E. L., and L. I. Krishtalik. 2000. Low dielectric response in enzyme active site. *Proc. Natl. Acad. Sci. USA.* 97:2081–2086.

Meyer, B., E. Schlodder, J. P. Dekker, and H. T. Witt. 1989. O_2 evolution and Chl a_{II}^+ (P-680$^+$) nanosecond reduction kinetics in single flashes as a function of pH. *Biochim. Biophys. Acta.* 974:36–43.

Moser, C. C., J. M. Keske, K. Warncke, R. S. Farid, and P. L. Dutton. 1992. Nature of biological electron transfer. *Nature.* 355:796–802.

Moser, C. C., C. C. Page, X. Chen, and P. L. Dutton. 1997. Biological electron tunneling through native protein media. *J. Biol. Inorg. Chem.* 2:393–398.

Mulkidjanian, A. Y. 1999. Conformationally controlled pK-switching in membrane proteins: one more mechanism specific to the enzyme catalysis? *FEBS Lett.* 463:199–204.

Mulkidjanian, A. Y., V. P. Shinkarev, M. I. Verkhovsky, and B. S. Kaurov. 1986. A study of kinetic properties of the stable semiquinone of the reaction center secondary acceptor in chromatophores of nonsulfur purple bacteria. *Biochim. Biophys. Acta.* 849:150–161.

Nadler, W., and R. A. Marcus. 1987. Dynamical effects in electron transfer reactions. II. Numerical solution. *J. Chem. Phys.* 86:3906–3924.

Nadler, W., and R. A. Marcus. 1988. Non-exponential time behavior of electron transfer in an inhomogeneous polar medium. *Chem. Phys. Lett.* 144:24–30.

Okamura, M. Y., M. L. Paddock, M. S. Graige, and G. Feher. 2000. Proton and electron transfer in bacterial reaction centers. *Biochim. Biophys. Acta.* 1458:148–163.

Ortega, J. M., and P. Mathis. 1992. Effect of temperature on the kinetics of electron transfer from the tetraheme cytochrome to the primary donor in *Rhodopseudomonas viridis. FEBS Lett.* 301:45–48.

Ortega, J. M., and P. Mathis. 1993. Electron transfer from the tetraheme cytochrome to the special pair in isolated reaction centers of *Rhodopseudomonas viridis. Biochemistry.* 32:1141–1151.

Ovchinnikova, M. Ya. 1981. The frequency factor in the rate constant of electron transfer reactions. *Teor. Eksp. Khim.* 17:651–654.

Paddock, M. L., G. Feher, and M. Y. Okamura. 2000. Identification of the proton pathway in bacterial reaction centers: replacement of Asp-M17 and Asp-L210 with Asn reduces the proton transfer rate in the presence of Cd_2^+. *Proc. Natl. Acad. Sci. USA.* 97:1548–1553.

Paddock, M. L., M. E. Senft, M. S. Graige, S. H. Rongey, T. Turanchik, G. Feher, and M. Y. Okamura. 1998. Characterization of second site mutations show that fast proton transfer to Q_B^- is restored in bacterial reaction centers of *Rhodobacter sphaeroides* containing the Asp-L213→Asn lesion. *Photosynth. Res.* 55:281–291.

Page, C. C., C. C. Moser, X. Chen, and P. L. Dutton. 1999. Natural engineering principles of electron tunnelling in biological oxidation–reduction. *Nature.* 402:47–52.

Parson, W. W. 1991. Reaction centers. *In* Chlorophylls. H. Scheer, editor. CRC Press, Boca Raton, FL. 1153–1180.

Parson, W. W., Z. T. Chu, and A. Warshel. 1998a. Oscillations of the energy gap for the initial electron-transfer step in bacterial reaction centers. *Photosynth. Res.* 55:147–152.

Parson, W. W., Z. T. Chu, and A. Warshel. 1998b. Reorganization energy of the initial electron-transfer step in photosynthetic bacterial reaction centers. *Biophys. J.* 74:182–191.

Peloquin, J. M., J. C. Williams, X. Lin, R. G. Alden, A. K. W. Taguchi, J. P. Allen, and N. W. Woodbury. 1994. Time-dependent thermodynamics during early electron transfer in reaction centers from *Rhodopseudomonas sphaeroides. Biochemistry.* 33:8089–8100.

Raineri, F. O., and H. L. Friedman. 1999. Solvent control of electron transfer reactions. *In* Electron Transfer: From Isolated Molecules to Biomolecules, Part 2. J. Jortner and M. Bixon, editors. John Wiley & Sons, New York. 81–189.

Rasaiah, J. C., and J. Zhu. 1993. An integral equation approximation for the dynamics of reverible electron-transfer reactions. *J. Chem. Phys.* 98: 1213–1227.

Rips, I., and J. Jortner. 1987a. Dynamic solvent effects on outer-sphere electron transfer. *J. Chem. Phys.* 87:2090–2104.

Rips, I., and J. Jortner. 1987b. Outer sphere electron transfer in polar solvents. Activationless and inverted regimes. *J. Chem. Phys.* 87: 6513–6519.

Rips, I., and J. Jortner. 1988. Activationless solvent-controlled electron transfer. *J. Chem. Phys.* 88:818–822.

Risken, H. 1996. The Fokker–Planck Equation. Methods of Solution and Applications. Springer-Verlag, Berlin.

Roy, S., and B. Bagchi. 1994. Time dependent solution of generalized Zusman model of outersphere electron transfer reactions: application to various experimental situations. *J. Chem. Phys.* 100:8802–8816.

Sagnella, D. E., and J. E. Straub. 1999. A study of vibrational relaxation of B-state carbon monoxide in the heme pocket of photolyzed carboxymyoglobin. *Biophys. J.* 77:70–84.

Sagnella, D. E., J. E. Straub, T. A. Jackson, M. Lim, and P. A. Anfinrud. 1999. Vibrational population relaxation of carbon monoxide in the heme pocket of photolyzed carbonmonoxy myoglobin: Comparison of time-resolved mid-IR absorbance experiments and molecular dynamics simulations. *Proc. Natl. Acad. Sci. USA.* 96:14324–14329.

Schilstra, M. J., F. Rappaport, J. H. Nugent, C. J. Barnett, and D. R. Klug. 1998. Proton/hydrogen transfer affects the S-state-dependent microsecond phases of P680$^+$ reduction during water splitting. *Biochemistry.* 37:3974–3981.

Sharp, R. E., and S. K. Chapman. 1999. Mechanisms for regulating electron transfer in multi-centre redox proteins. *Biochim. Biophys. Acta.* 1432:143–158.

Shinkarev, V. P., E. Takahashi, and C. A. Wraight. 1992. Electrostatic interactions and flash-induced proton uptake in reaction centers from *Rb. sphaeroides. In* The Photosynthetic Bacterial Reaction Center II. J. Breton and A. Vermeglio, editors. Plenum Press, New York. 375–387.

Shopes, R. J., and C. A. Wraight. 1987. Charge recombination from the $P^+Q_A^-$ state in reaction centers from *Rhodopseudomonas viridis. Biochim. Biophys. Acta.* 893:409–425.

Spörlein, S., W. Zinth, and J. Wachtveitl. 1998. Vibrational coherence in photosynthetic reaction centers observed in the bacteriochlorophyll anion band. *J. Phys. Chem. B.* 102:7492–7496.

Stowell, M. H., T. M. Mcphillips, D. C. Rees, S. M. Soltis, E. Abresch, and G. Feher. 1997. Light-induced structural changes in photosynthetic reaction center: implications for mechanism of electron–proton transfer. *Science.* 276:812–816.

Streltsov, A. M., T. J. Aartsma, A. J. Hoff, and V. A. Shuvalov. 1997. Oscillations within the B_L absorption band of *Rhodobacter sphaeroides* reaction centers upon 30 femtosecond excitation at 865 nm. *Chem. Phys. Lett.* 266:347–352.

Streltsov, A. M., S. I. E. Vulto, A. Y. Shkuropatov, A. J. Hoff, T. J. Aartsma, and V. A. Shuvalov. 1998. B_A and B_B absorbance perturbations induced by coherent nuclear motions in reaction centers from *Rhodobacter sphaeroides* upon 30-fs excitation of the primary donor. *J. Phys. Chem. B.* 102:7293–7298.

Sumi, H., and R. A. Marcus. 1986. Dynamical effects in electron transfer reactions. *J. Chem. Phys.* 84:4894–4914.

Takahashi, E., P. Maroti, and C. A. Wraight. 1992. Coupled proton and electron transfer pathways in the acceptor quinone complex of reaction centers from *Rhodobacter sphaeroides. In* Electron and Proton Transfer in Chemistry and Biology. A. Müller, E. Diemann, W. Junge, and H. Ratajczak, editors. Elsevier, Amsterdam. 219–236.

Takahashi, E., and C. A. Wraight. 1992. Proton and electron transfer in the acceptor quinone complex of *Rhodobacter sphaeroides* reaction centers: characterization of site-directed mutants of the two ionizable residues, Glu^{L212} and Asp^{L213}, in the Q_B binding site. *Biochemistry.* 31:855–866.

Tiede, D. M., L. Utschig, D. K. Hanson, and D. M. Gallo. 1998. Resolution of electron and proton transfer events in the electrochromism associated with quinone reduction in bacterial reaction centers. *Photosynth. Res.* 55:267–273.

Tiede, D. M., J. Vazquez, J. Cordova, and P. A. Marone. 1996. Time-resolved electrochromism associated with the formation of quinone anions in the *Rhodobacter sphaeroides* R26 reaction center. *Biochemistry.* 35:10763–10775.

Ulstrup, J. 1979. Charge Transfer in Condensed Media. Springer, Berlin.

Vos, M. H., and J. L. Martin. 1999. Femtosecond processes in proteins. *Biochim. Biophys. Acta.* 1411:1–20.

Vos, M. H., C. Rischel, M. R. Jones, and J. L. Martin. 2000. Electrochromic detection of a coherent component in the formation of the charge pair $P^+H_L^-$ in bacterial reaction centers. *Biochemistry.* 39:8353–8361.

Warshel, A., Z. T. Chu, and W. W. Parson. 1989. Dispersed polaron simulations of electron transfer in photosynthetic reaction centers. *Science.* 246:112–116.

Warshel, A., and S. T. Russell. 1984. Calculations of electrostatic interactions in biological systems and in solutions. *Quart. Rev. Biophys.* 17: 283–422.

Woutersen, S., and H. J. Bakker. 1999. Resonant intermolecular transfer of vibrational energy in liquid water. *Nature.* 402:507–509.

Wraight, C. A. 1979. Electron acceptors of bacterial photosynthetic reaction centers. II. Proton binding coupled to secondary electron transfer in the quinone acceptor complex. *Biochim. Biophys. Acta.* 548:309–327.

Xu, D., and K. Schulten. 1994. Coupling of protein motion to electron transfer in a photosynthetic reaction center: investigating the low temperature behavior in the framework of the spin-boson model. *Chem. Phys.* 182:91–117.

Yakobson, B. I., and A. I. Burshtein. 1980. Relaxation hindrance in nonadiabatic cage reactions. *Chem. Phys.* 11:385–395.

Yakovlev, A. G., A. Y. Shkuropatov, and V. A. Shuvalov. 2000. Nuclear wavepacket motion producing a reversible charge separation in bacterial reaction centers. *FEBS Lett.* 466:209–212.

Yruela, I., M. S. Churio, T. Gensch, S. E. Braslavsky, and A. R. Holzwarth. 1994. Optoacoustic and singlet oxygen near-IR emission study of the isolated D1–D2-Cyt b_{559} reaction-center complex of photosystem II. Protein movement associated with charge separation. *J. Phys. Chem.* 98:12789–12795.

Zhu, J., and J. C. Rasaiah. 1991. Dynamics of reversible electron transfer reactions. *J. Chem. Phys.* 95:3325–3340.

Zhu, J., and J. C. Rasaiah. 1992. Reversible electron transfer dynamics in non-Debye solvents. *J. Chem. Phys.* 96:1435–1443.

Zhu, J., and J. C. Rasaiah. 1994. Solvent dynamical effects on electron transfer reactions. *J. Chem. Phys.* 101:9966–9981.

Zusman, L. D. 1980. Outer-sphere electron transfer in polar solvents. *Chem. Phys.* 49:295–304.

Zusman, L. D. 1988. The theory of electron transfer reactions in solvents with two characteristic relaxation times. *Chem. Phys.* 119:51–61.